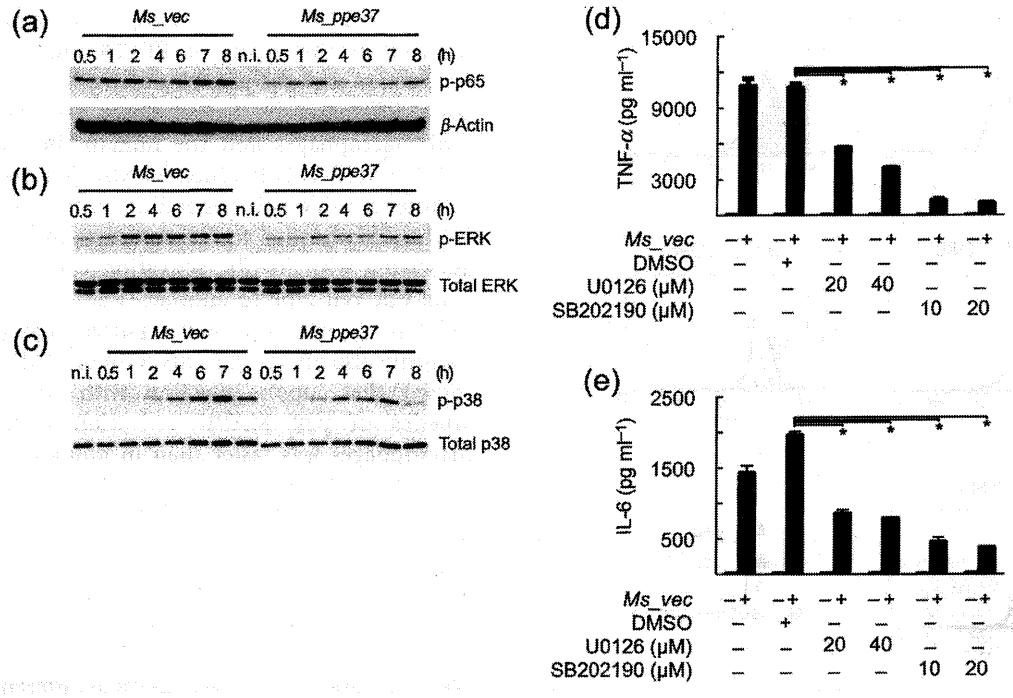

Fig. 6. Phosphorylation of the NF-κB p65 subunit, ERK and p38 in macrophages infected with recombinant *M. smegmatis*. (a–c) Peritoneal exudate macrophages were infected with Ms_ppe37 or Ms_vec at an m.o.i. of 20. Macrophages were washed and lysed after 0.5, 1, 2, 4, 6, 7 and 8 h of infection. Lysates were subjected to Western blot analyses to detect the phosphorylated NF-κB p65 subunit (p-p65) (a), phosphorylated ERK (p-ERK) (b) and phosphorylated p38 (p-p38) (c) with specific antibodies. Detection of β-actin, total ERK and total p38 indicated equal protein loading. Similar results were obtained in three independent experiments. n.i, No infection. (d, e) Peritoneal exudate macrophages were treated with U0126 (a MEK1/2 inhibitor) or SB202190 (a p38 inhibitor) at the indicated concentrations. Treatment with DMSO served as a control for the inhibitor treatments. After 1 h, the macrophages were infected with Ms_vec at an m.o.i. of 20. Culture supernatants were harvested after 24 h of infection and the concentrations of TNF-α (d) and IL-6 (e) in the culture supernatants were determined. Data are shown as means ± SD of triplicate wells. *, $P<0.05$ by Student's two-tailed *t*-test. Similar results were obtained in three independent experiments. −, No infection or treatment; +, with infection or treatment.

activation of MAPKs and NF-κB. However, TLR2 is not the only candidate receptor with the possibility of interacting with PPE37, as the common activation of the MAPK and NF-κB signalling pathways is not limited to this receptor alone.

In the context of *M. tuberculosis* infection, the possible role of PPE37 in interfering with the pro-inflammatory cytokine response in infected macrophages might also be applicable. Manca *et al.* (1999) reported that infection of human monocytes with *M. tuberculosis* clinical isolate CDC1551 induced a higher level of TNF-α, IL-6 and IL-12 than infection with the *M. tuberculosis* laboratory strain H37Rv. It may be possible that this vigorous pro-inflammatory cytokine response induced by CDC1551 was due in part to the loss of PPE37 function. Comparative genome analysis between CDC1551 and H37Rv has revealed that the *ppe37* gene is deleted from the genome of CDC1551 (Gey van Pittius *et al.*, 2006).

In conclusion, the present study suggests that the *M. tuberculosis* PPE37 may have a role in interfering with the pro-inflammatory cytokine response in macrophages infected with *M. smegmatis*. It is established that pro-inflammatory cytokines such as TNF-α (Elbek *et al.*, 2009; Flynn *et al.*, 1995; Jacobs *et al.*, 2007; Lin *et al.*, 2007; Wolfe *et al.*, 2004) are critical to host immune responses in containing *M. tuberculosis* infection. Subversion and modulation of the host inflammatory response can thus be an advantageous pathogenic strategy for *M. tuberculosis*. In light of the possible role of PPE37 suggested by our study, a hypothesis of the possible contribution of PPE37 to such a pathogenesis strategy is presented. Our results thus provide a basis to investigate and characterize further the role of PPE37 in the context of *M. tuberculosis* infection. Future studies that are needed include the construction and testing of knockout genes in *M. tuberculosis*.

ACKNOWLEDGEMENTS

This study was supported by a grant-in-aid for scientific research on priority areas from the Ministry of Education, Science, Culture and

Sports of Japan, grants-in-aid for scientific research (B and C), a grant-in-aid for young scientists (B) from the Japan Society for the Promotion of Science, a grant-in-aid for research on emerging and re-emerging infectious disease from the Ministry of Health, Labour and Welfare of Japan, and a grant-in-aid from the Waksman Foundation of Japan.

REFERENCES

Adindla, S. & Guruprasad, L. (2003). Sequence analysis corresponding to the PPE and PE proteins in *Mycobacterium tuberculosis* and other genomes. *J Biosci* **28**, 169–179.

Akira, S., Yamamoto, M. & Takeda, K. (2003). Role of adapters in Toll-like receptor signalling. *Biochem Soc Trans* **31**, 637–642.

Behar, S. M., Divangahi, M. & Remold, H. G. (2010). Evasion of innate immunity by *Mycobacterium tuberculosis*: is death an exit strategy? *Nat Rev Microbiol* **8**, 668–674.

Bentley, W. E., Mirjalili, N., Andersen, D. C., Davis, R. H. & Kompala, D. S. (1990). Plasmid-encoded protein: the principal factor in the "metabolic burden" associated with recombinant bacteria. *Biotechnol Bioeng* **35**, 668–681.

Chapin, K. C. & Lauderdale, T.-L. (2007). Reagents, stains, and media: bacteriology. In *Manual of Clinical Microbiology*, 9th edn, pp. 334–364. Edited by P. R. Murray, E. J. Baron, J. H. Jorgensen, M. L. Landry & M. A. Pfaller. Washington, DC: American Society for Microbiology.

Choudhary, R. K., Mukhopadhyay, S., Chakhaiyar, P., Sharma, N., Murthy, K. J. R., Katoch, V. M. & Hasnain, S. E. (2003). PPE antigen Rv2430c of *Mycobacterium tuberculosis* induces a strong B-cell response. *Infect Immun* **71**, 6338–6343.

Cole, S. T., Brosch, R., Parkhill, J., Garnier, T., Churcher, C., Harris, D., Gordon, S. V., Eiglmeier, K., Gas, S. & other authors (1998). Deciphering the biology of *Mycobacterium tuberculosis* from the complete genome sequence. *Nature* **393**, 537–544.

Collart, M. A., Baeuerle, P. & Vassalli, P. (1990). Regulation of tumor necrosis factor alpha transcription in macrophages: involvement of four κB-like motifs and of constitutive and inducible forms of NF-κB. *Mol Cell Biol* **10**, 1498–1506.

Divangahi, M., Desjardins, D., Nunes-Alves, C., Remold, H. G. & Behar, S. M. (2010). Eicosanoid pathways regulate adaptive immunity to *Mycobacterium tuberculosis*. *Nat Immunol* **11**, 751–758.

Elbek, O., Uyar, M., Aydin, N., Börekçi, S., Bayram, N., Bayram, H. & Dikensoy, Ö. (2009). Increased risk of tuberculosis in patients treated with antitumor necrosis factor alpha. *Clin Rheumatol* **28**, 421–426.

Faggioli, L., Costanzo, C., Donadelli, M. & Palmieri, M. (2004). Activation of the interleukin-6 promoter by a dominant negative mutant of c-Jun. *Biochim Biophys Acta* **1692**, 17–24.

Flynn, J. L., Goldstein, M. M., Chan, J., Triebold, K. J., Pfeffer, K., Lowenstein, C. J., Schreiber, R., Mak, T. W. & Bloom, B. R. (1995). Tumor necrosis factor-α is required in the protective immune response against *Mycobacterium tuberculosis* in mice. *Immunity* **2**, 561–572.

Gardy, J. L. & Brinkman, F. S. L. (2006). Methods for predicting bacterial protein subcellular localization. *Nat Rev Microbiol* **4**, 741–751.

Gey van Pittius, N. C., Sampson, S. L., Lee, H., Kim, Y., van Helden, P. D. & Warren, R. M. (2006). Evolution and expansion of the *Mycobacterium tuberculosis* PE and PPE multigene families and their association with the duplication of the ESAT-6 (*esx*) gene cluster regions. *BMC Evol Biol* **6**, 95.

Gordon, S. V., Eiglmeier, K., Brosch, R., Garnier, T., Honore, N., Barrell, B. & Cole, S. T. (1999). Genomics of *Mycobacterium tuberculosis* and *Mycobacterium leprae*. In *Mycobacteria Molecular Biology and Virulence*, pp. 93–109. Edited by C. Ratledge & J. Dale. Oxford: Blackwell Science.

Gutierrez, M. G., Mishra, B. B., Jordao, L., Elliott, E., Anes, E. & Griffiths, G. (2008). NF-κB activation controls phagolysosome fusion-mediated killing of mycobacteria by macrophages. *J Immunol* **181**, 2651–2663.

Jacobs, M., Togbe, D., Fremond, C., Samarina, A., Allie, N., Botha, T., Carlos, D., Parida, S. K., Grivennikov, S. & Nedospasov, S. (2007). Tumor necrosis factor is critical to control tuberculosis infection. *Microbes Infect* **9**, 623–628.

Jo, E.-K., Yang, C.-S., Choi, C. H. & Harding, C. V. (2007). Intracellular signalling cascades regulating innate immune responses to *Mycobacteria*: branching out from Toll-like receptors. *Cell Microbiol* **9**, 1087–1098.

Khan, N., Alam, K., Nair, S., Valluri, V. L., Murthy, K. J. R. & Mukhopadhyay, S. (2008). Association of strong immune responses to PPE protein Rv1168c with active tuberculosis. *Clin Vaccine Immunol* **15**, 974–980.

Kuprash, D. V., Udalova, I. A., Turetskaya, R. L., Kwiatkowski, D., Rice, N. R. & Nedospasov, S. A. (1999). Similarities and differences between human and murine TNF promoters in their response to lipopolysaccharide. *J Immunol* **162**, 4045–4052.

Larsen, M. H. (2000). Some common methods in mycobacterial genetics. In *Molecular Genetics of Mycobacteria*, pp. 319–320. Edited by G. F. Hatfull & W. R. Jacobs, Jr. Washington, DC: American Society for Microbiology.

Lee, S.-B. & Schorey, J. S. (2005). Activation and mitogen-activated protein kinase regulation of transcription factors Ets and NF-κB in mycobacterium-infected macrophages and role of these factors in tumor necrosis factor alpha and nitric oxide synthase 2 promoter function. *Infect Immun* **73**, 6499–6507.

Libermann, T. A. & Baltimore, D. (1990). Activation of interleukin-6 gene expression through the NF-κB transcription factor. *Mol Cell Biol* **10**, 2327–2334.

Lin, P. L., Plessner, H. L., Voitenok, N. N. & Flynn, J. L. (2007). Tumor necrosis factor and tuberculosis. *J Investig Dermatol Symp Proc* **12**, 22–25.

Manca, C., Tsenova, L., Barry, C. E., III, Bergtold, A., Freeman, S., Haslett, P. A. J., Musser, J. M., Freedman, V. H. & Kaplan, G. (1999). *Mycobacterium tuberculosis* CDC1551 induces a more vigorous host response in vivo and in vitro, but is not more virulent than other clinical isolates. *J Immunol* **162**, 6740–6746.

Nair, S., Ramaswamy, P. A., Ghosh, S., Joshi, D. C., Pathak, N., Siddiqui, I., Sharma, P., Hasnain, S. E., Mande, S. C. & Mukhopadhyay, S. (2009). The PPE18 of *Mycobacterium tuberculosis* interacts with TLR2 and activates IL-10 induction in macrophage. *J Immunol* **183**, 6269–6281.

Post, F. A., Manca, C., Neyrolles, O., Ryffel, B., Young, D. B. & Kaplan, G. (2001). *Mycobacterium tuberculosis* 19-kilodalton lipoprotein inhibits *Mycobacterium smegmatis*-induced cytokine production by human macrophages in vitro. *Infect Immun* **69**, 1433–1439.

Rao, K. M. K. (2001). MAP kinase activation in macrophages. *J Leukoc Biol* **69**, 3–10.

Roach, S. K. & Schorey, J. S. (2002). Differential regulation of the mitogen-activated protein kinases by pathogenic and nonpathogenic mycobacteria. *Infect Immun* **70**, 3040–3052.

Roach, S. K., Lee, S.-B. & Schorey, J. S. (2005). Differential activation of the transcription factor cyclic AMP response element binding protein (CREB) in macrophages following infection with pathogenic and nonpathogenic mycobacteria and role for CREB in tumor necrosis factor alpha production. *Infect Immun* **73**, 514–522.

Rodriguez, G. M., Gold, B., Gomez, M., Dussurget, O. & Smith, I. (1999). Identification and characterization of two divergently transcribed iron regulated genes in *Mycobacterium tuberculosis*. *Tuber Lung Dis* **79**, 287–298.

Rodriguez, G. M., Voskuil, M. I., Gold, B., Schoolnik, G. K. & Smith, I. (2002). *ideR*, an essential gene in *Mycobacterium tuberculosis*: role of IdeR in iron-dependent gene expression, iron metabolism, and oxidative stress response. *Infect Immun* **70**, 3371–3381.

Romano, M., Rindi, L., Korf, H., Bonanni, D., Adnet, P. Y., Jurion, F., Garzelli, C. & Huygen, K. (2008). Immunogenicity and protective efficacy of tuberculosis subunit vaccines expressing PPE44 (Rv2770c). *Vaccine* **26**, 6053–6063.

Rosenkrands, I. & Andersen, P. (2001). Preparation of culture filtrate proteins from *Mycobacterium tuberculosis*. In *Mycobacterium tuberculosis Protocols*, pp. 205–215. Edited by T. Parish & N. G. Stoker. Totowa, NJ: Humana Press.

Schnappinger, D., Ehrt, S., Voskuil, M. I., Liu, Y., Mangan, J. A., Monahan, I. M., Dolganov, G., Efron, B., Butcher, P. D. & other authors (2003). Transcriptional adaptation of *Mycobacterium tuberculosis* within macrophages: insights into the phagosomal environment. *J Exp Med* **198**, 693–704.

Stover, C. K., de la Cruz, V. F., Fuerst, T. R., Burlein, J. E., Benson, L. A., Bennett, L. T., Bansal, G. P., Young, J. F., Lee, M. H. & other authors (1991). New use of BCG for recombinant vaccines. *Nature* **351**, 456–460.

Surewicz, K., Aung, H., Kanost, R. A., Jones, L., Hejal, R. & Toossi, Z. (2004). The differential interaction of p38 MAP kinase and tumor necrosis factor-α in human alveolar macrophages and monocytes induced by *Mycobacterium tuberculosis*. *Cell Immunol* **228**, 34–41.

Tundup, S., Pathak, N., Ramanadham, M., Mukhopadhyay, S., Murthy, K. J. R., Ehtesham, N. Z. & Hasnain, S. E. (2008). The co-operonic PE25/PPE41 protein complex of *Mycobacterium tuberculosis* elicits increased humoral and cell mediated immune response. *PLoS ONE* **3**, e3586.

Voskuil, M. I., Schnappinger, D., Rutherford, R., Liu, Y. & Schoolnik, G. K. (2004). Regulation of the *Mycobacterium tuberculosis* PE/PPE genes. *Tuberculosis (Edinb)* **84**, 256–262.

Wang, J., Qie, Y., Zhang, H., Zhu, B., Xu, Y., Liu, W., Chen, J. & Wang, H. (2008). PPE protein (Rv3425) from DNA segment RD11 of *Mycobacterium tuberculosis*: a novel immunodominant antigen of *Mycobacterium tuberculosis* induces humoral and cellular immune responses in mice. *Microbiol Immunol* **52**, 224–230.

Wolfe, F., Michaud, K., Anderson, J. & Urbansky, K. (2004). Tuberculosis infection in patients with rheumatoid arthritis and the effect of infliximab therapy. *Arthritis Rheum* **50**, 372–379.

Zhang, Y., Broser, M. & Rom, W. N. (1994). Activation of the interleukin 6 gene by *Mycobacterium tuberculosis* or lipopolysaccharide is mediated by nuclear factors NF-IL6 and NF-κB. *Proc Natl Acad Sci U S A* **91**, 2225–2229.

ANTIMICROBIAL AGENTS AND CHEMOTHERAPY, Aug. 2011, p. 3661–3667 Vol. 55, No. 8
0066-4804/11/$12.00 doi:10.1128/AAC.00042-11

Impact of the E540V Amino Acid Substitution in GyrB of *Mycobacterium tuberculosis* on Quinolone Resistance[▽]†

Hyun Kim,[1] Chie Nakajima,[1] Kazumasa Yokoyama,[1] Zeaur Rahim,[2] Youn Uck Kim,[3] Hiroki Oguri,[4] and Yasuhiko Suzuki[1,5]*

Department of Global Epidemiology, Hokkaido University Research Center for Zoonosis Control, Sapporo 001-0020, Japan[1]; Tuberculosis Laboratory, International Center for Diarrheal Disease Research, Bangladesh, Dhaka 1000, Bangladesh[2]; Department of Biomedical Sciences, Sun Moon University, A-San 336-708, Republic of Korea[3]; Division of Chemistry, Graduate School of Science, and Division of Innovative Research, Creative Research Institution (CRIS), Hokkaido University, North 21, West 10, Kita-ku, Sapporo 001-0021, Japan[4]; and JST/JICA-SATREPS, Tokyo 120-8666, Japan[5]

Received 11 January 2011/Returned for modification 8 February 2011/Accepted 20 May 2011

Amino acid substitutions conferring resistance to quinolones in *Mycobacterium tuberculosis* have generally been found within the quinolone resistance-determining regions (QRDRs) in the A subunit of DNA gyrase (GyrA) rather than the B subunit of DNA gyrase (GyrB). To clarify the contribution of an amino acid substitution, E540V, in GyrB to quinolone resistance in *M. tuberculosis*, we expressed recombinant DNA gyrases in *Escherichia coli* and characterized them *in vitro*. Wild-type and GyrB-E540V DNA gyrases were reconstituted *in vitro* by mixing recombinant GyrA and GyrB. Correlation between the amino acid substitution and quinolone resistance was assessed by the ATP-dependent DNA supercoiling assay, quinolone-inhibited supercoiling assay, and DNA cleavage assay. The 50% inhibitory concentrations of eight quinolones against DNA gyrases bearing the E540V amino acid substitution in GyrB were 2.5- to 36-fold higher than those against the wild-type enzyme. Similarly, the 25% maximum DNA cleavage concentrations were 1.5- to 14-fold higher for the E540V gyrase than for the wild-type enzyme. We further demonstrated that the E540V amino acid substitution influenced the interaction between DNA gyrase and the substituent(s) at R-7, R-8, or both in quinolone structures. This is the first detailed study of the contribution of the E540V amino acid substitution in GyrB to quinolone resistance in *M. tuberculosis*.

A major human infectious disease, tuberculosis (TB) is estimated to affect approximately one-third of the world's population, and 95% of cases occur in developing countries (15, 30, 31). Current estimates show that approximately 9.4 million new cases and nearly 1.7 million deaths from TB occur each year, and TB remains a major cause of premature death (36).

The increased incidence of multidrug-resistant (MDR) TB (TB resistant to more than two anti-TB drugs, including rifampin and isoniazid [35]) has hampered the treatment and control of TB and is associated with an increase in mortality rates in people with TB (3, 37, 40). Consequently, the required drug dosage for the treatment of TB has dramatically increased (38), and fluoroquinolones (FQs) are now considered to be important second-line anti-TB agents (13, 20).

FQs are a large and widely used class of synthetic antibacterial agents (10, 11, 21, 39) which are frequently used in treating patients infected with MDR TB (6, 17, 22). The target of the FQs in *Mycobacterium tuberculosis* is DNA gyrase, which consists of two subunits, GyrA and GyrB, that form the catalytically active $GyrA_2GyrB_2$ heterotetrameric structure (7, 9, 18). DNA gyrase is an ATP-dependent enzyme that transiently cleaves and unwinds double-stranded DNA (9) to catalyze the negative supercoiling of DNA and is thus essential for efficient DNA replication, transcription, and recombination (7, 24, 29). Most eubacteria, such as *Escherichia coli*, have two DNA topoisomerases, DNA gyrase and topoisomerase IV. A few bacteria, however, such as *M. tuberculosis*, have only DNA gyrase (8), which is therefore the sole target of quinolones.

The quinolone-binding sites in DNA gyrase have been found to be in the quinolone resistance-determining regions (QRDRs) in the GyrA subunit (amino acids Gly-88 to Asp-94 in *M. tuberculosis*) and the GyrB subunit (amino acids Asp-500 to Asn-538 in *M. tuberculosis*), which contain the majority of the amino acid substitutions that confer quinolone resistance (Fig. 1) (2, 19, 27, 32, 33). A recent study using three-dimensional structure analysis, however, has suggested that QRDRs of *M. tuberculosis* gyrase are located at amino acids Ser-73 to Gln-113 of the GyrA subunit and Asn-493 to Asn-540 of the GyrB subunit (28). The QRDRs in GyrB are thought to interact with those in GyrA and DNA strands to form a quinolone-binding pocket (QBP).

In this study, we elucidated the contribution of an amino acid substitution located at position 540 that is found in a quinolone-resistant clinical isolate by *in vitro* DNA supercoiling and cleavage assays in the presence or absence of FQs. We also propose the mechanism of interaction between substituents of FQs and amino acid residues in the QBP of GyrB.

MATERIALS AND METHODS

Reagents and kits. Gatifloxacin (GAT), levofloxacin (LVX), ciprofloxacin (CIP), sparfloxacin (SPX), and enoxacin (ENX) were purchased from LKT Laboratories, Inc. (St. Paul, MN); sitafloxacin (SIX) was from Daiichi Pharma-

* Corresponding author. Mailing address: Department of Global Epidemiology, Hokkaido University Research Center for Zoonosis Control, Kita 20-Nishi 10, Kita-ku, Sapporo 001-0020, Japan. Phone: 81-11-706-9503. Fax: 81-11-706-7310. E-mail: suzuki@czc.hokudai.ac.jp.

† Supplemental material for this article may be found at http://aac.asm.org/.

▽ Published ahead of print on 6 June 2011.

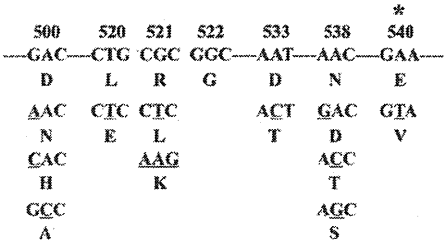

FIG. 1. Amino acid substitutions found within the QRDR of GyrB in FQ-resistant *M. tuberculosis*. The amino acid substitutions are shown below the nucleotide sequence. The target nucleotide substitution of this study is denoted by the asterisk, and mutated bases are underlined.

ceutical, Co., Ltd. (Tokyo, Japan); norfloxacin (NOR) was from Wako Pure Chemical Industries, Ltd. (Tokyo, Japan); moxifloxacin (MXF) was from Toronto Research Chemicals Inc. (Ontario, Canada); and ampicillin was from Meiji Seika Kaisha, Ltd. (Tokyo, Japan). Oligonucleotide primers were synthesized by Life Technologies (Carlsbad, CA). TOPO TA cloning (pCR 4-TOPO) and Ni-nitrilotriacetic acid protein purification kits were purchased from Life Technologies. Restriction enzymes were obtained from New England BioLabs, Inc. (Ipswich, MA). The supercoiling assay kit and supercoiled and relaxed pBR322 DNA were purchased from John Innes Enterprises Ltd. (Norwich, United Kingdom). Protease inhibitor cocktail (Complete Mini, EDTA free) was purchased from Roche Applied Science (Mannheim, Germany).

Bacterial strains and plasmids. *E. coli* strain TOP-10 (Life Technologies) was used as the host for cloning purposes. *E. coli* strains Rosetta-gami 2 and BL21(DE3)/pLysS were purchased from Merck KGaA (Darmstadt, Germany) and used for protein expression. Vector plasmids pET-20b (+) and pET-19b (Merck KGaA) were used to construct expression plasmids for *M. tuberculosis* proteins GyrA and GyrB, respectively.

Construction of wild-type (WT) and GyrB-E540V DNA gyrase expression vectors. The construction of WT DNA gyrase expression vectors is shown in Fig. S1 in the supplemental material. A nucleotide substitution was introduced into the *M. tuberculosis* WT *gyrB* gene by PCR with pairs of complementary primers containing the nucleotide substitution of interest (Table 1). The *gyrB*-M cassettes with mutated bases were amplified from the WT *gyrB* gene cassette (see Fig. S1C in the supplemental material) and ligated into the TA cloning plasmid. Recombinant plasmids were recovered from the colonies, and a nucleotide substitution in QRDRs in the 294-base PCR products was confirmed. The *gyrB*-M cassettes were digested with SacI and HindIII, ligated into pTB-B digested with same restriction endonucleases, and transformed into *E. coli* TOP-10 to obtain GyrB-E540V expression plasmids. Recombinant clones were selected from the resistant colonies on LB agar plates containing ampicillin (100 μg/ml).

Sequencing of products. PCR products were purified by agarose gel electrophoresis. The agarose blocks containing the bands of interest were sliced out of the agarose gel, frozen at −80°C for 30 min, and centrifuged at 20,400 × *g* at 4°C for 10 min to collect the supernatants. Supernatants having DNA concentrations between approximately 10 and 20 ng/μl were used directly as templates for cycle sequencing in both directions with corresponding primers (0.10 μmol) using the ABI Prism BigDye Terminator v3.1 cycle sequencing kit (Applied Biosystems, Foster City, CA). The sequencing reactions were performed according to the manufacturer's instructions. Cycle sequencing products were subsequently analyzed on an ABI PRISM 3130x automated genetic analyzer (Applied Biosystems). The sequences generated with the program were compared to their respective WT and GyrB-E540V sequences using BioEdit software.

Recombinant expression and purification of DNA gyrase. DNA gyrase subunits were purified as previously described, with the following modifications (1, 2). Expression vectors carrying the *gyrA* and *gyrB* genes of *M. tuberculosis* were transformed into *E. coli* Rosetta-gami 2 and BL21(DE3)/pLysS, respectively. Expression of GyrA and GyrB was induced with the addition of 1 mM isopropyl-β-D-thiogalactopyranoside (IPTG; Wako Pure Chemicals Ltd.), followed by further incubation at 14°C for 20 h or at 23°C for 5 h, respectively. Combined elution fractions resulting from the addition of elution buffer (20 mM Tris-HCl [pH 8.0], 500 mM NaCl, 250 mM imidazole) to nickel-nitrilotriacetic acid agarose resin (Invitrogen) were dialyzed twice overnight at 4°C against 1 liter of gyrase dilution buffer (50 mM Tris-HCl [pH 7.5], 100 mM KCl, 2 mM dithiothreitol, 1 mM EDTA). After dialysis, the eluates were added to glycerol to yield 50% (wt/vol) and stored at −80°C until use. The protein fractions were examined by sodium dodecyl sulfate (SDS)-polyacrylamide gel electrophoresis.

DNA supercoiling assay and inhibition by FQs. ATP-dependent DNA supercoiling and quinolone-inhibited supercoiling assays were carried out as previously described (1, 2, 25). DNA supercoiling activity was tested with a combination of purified *M. tuberculosis* GyrA and GyrB proteins. The reaction mixture (total volume, 30 μl) consisted of DNA gyrase assay buffer, relaxed pBR322 DNA (0.3 μg), and WT and GyrB-E540V gyrase proteins (3 μM). Reactions were run at 37°C for 1 h and stopped by the addition of 30 μl of chloroform-isoamyl alcohol (24:1 mixture) and 6 μl of 5× stop and loading solution. The total reaction mixtures were subjected to electrophoresis in 1% agarose gels in 0.5× Tris-borate-EDTA (TBE) buffer. The gels were run for 1 h at 50 mA and stained with ethidium bromide (0.7 μg/ml). *E. coli* DNA gyrase (John Innes Enterprises Ltd.) was used as a positive control for the assay procedures and buffer. The inhibitory effects of quinolones on DNA gyrase were assessed by determining the drug concentrations required to inhibit the supercoiling activity of the enzyme by 50% (IC_{50}s) in the presence or absence of serial 2-fold increases in the concentrations of the eight FQs. Supercoiling activity was assessed by tracing the brightness of the bands corresponding to the supercoiled pBR322 DNA with the Molecular Analyst software ImageJ (http://rsbweb.nih.gov/ij). To allow direct comparison, all incubations with WT and GyrB-E540V enzymes were carried out and processed in parallel on the same day under identical conditions. All enzyme assays were performed at least three times to confirm reproducibility.

Quinolone-mediated DNA cleavage assay. DNA cleavage assays were carried out as previously described (1, 2, 25). Supercoiled, rather than relaxed, pBR322 DNA was used as the substrate for cleavage assays. The reaction mixture (total volume, 30 μl) contained DNA gyrase assay buffer, purified DNA gyrase subunits, supercoiled pBR322 DNA (0.3 μg), and increasing concentrations of GAT, LVX, CIP, MXF, SPX, or SIX. After incubation for 1 h at 37°C, 3 μl of 2% SDS and 3 μl of proteinase K (1 mg/ml) were added to the reaction mixture. After additional incubation for 30 min at 37°C, reactions were stopped to allow relaxation activity by the addition of 3 μl of 0.5 mM EDTA. 30 μl of chloroform-

TABLE 1. Oligonucleotide sequences of primers used in PCR

Primer	Sequence (nucleotide position), underlined element(s)	Comment
ON-873	5′-CCCATATGACAGACACGACGTTGCCGCC-3′ (1–23), NdeI site	WT *gyrA*
ON-874	5′-GTTAACCGGGCTTCGGTGTACCTCATCG-3′ (377–404), HpaI site	WT *gyrA*
ON-875	5′-GGTTAACCCCGTTGGCGATGGAGATGC-3′ (398–424), HpaI site	WT *gyrA*
ON-876	5′-GGCTCGAGTTAATGATGATGATGATGATGATTGCCCGTCTGGTCTGCGCCG-3′ (2493–2517), XhoI site and 6-histidine tag, respectively	WT *gyrA*
ON-35	5′-CCCCCCCATATGGGTAAAAACGAGGCCAGAAG-3′ (1–23), NdeI site	WT *gyrB*
ON-882	5′-CACGAGCTCTCGTGCCTTACGTGCCGCGATACG-3′ (1366–1398), SacI site	WT *gyrB*
ON-883	5′-GAGAGCTCGTGCGGCGTAAGAGCGCCACCG-3′ (1388–1417)	WT *gyrB*
ON-884	5′-CGATCTTGTGGTAGCGAAGCTTGCCGATATCGA-3′ (1667–1699), HindIII site	WT *gyrB*
ON-885	5′-CGATATCGGCAAGCTTCGCTACCACAAGATCG-3′ (1668–1699)	WT *gyrB*
ON-886	5′-GGCTCGAGTTAGACATCCAGGAACCGAACATCC-3′ (2130–2145), XhoI site	WT *gyrB*
ON-40	5′-AAAGAACACCGTAGTTCAGGCGA-3′ (1607–1630)[a]	Mutant *gyrB*
ON-41	5′-TCGCCTGAACTACGGTGTTCTTT-3′ (1607–1630)[a]	Mutant *gyrB*

[a] Mutated codon shown in bold type.

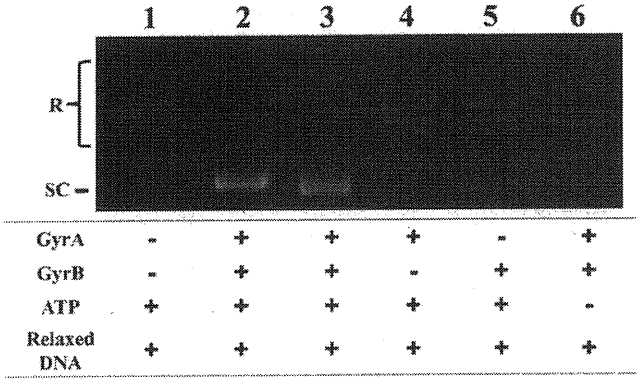

FIG. 2. Recombinant WT GyrA and GyrB subunits of *M. tuberculosis* generate an ATP-dependent DNA supercoiling activity. Relaxed pBR322 DNA (0.3 μg) was incubated with WT DNA gyrase reconstituted from GyrA (3 μM) and GyrB (3 μM) in the presence and absence of 1 mM ATP. The reactions were stopped, and the DNA products were separated by electrophoresis in 1% agarose gels. DNA was stained with ethidium bromide and photographed under UV illumination. Lane 1, relaxed pBR322 DNA; lane 2, relaxed pBR322 DNA and *E. coli* DNA gyrase; lane 3, relaxed pBR322 DNA and both recombinant GyrA and GyrB proteins; lane 4, relaxed pBR322 DNA and only GyrA protein; lane 5, relaxed pBR322 DNA and only GyrB protein; lane 6, absence of ATP. R and SC, relaxed and supercoiled pBR322 DNA, respectively.

isoamyl alcohol (24:1 mixture), and 3 μl of 10× DNA loading solution. Plasmid pBR322 linearized by BamHI digestion was used as a marker for cleaved DNA. The total reaction mixtures were subjected to electrophoresis in 0.8% agarose gels in 0.5× TBE buffer. The gels were run for 1.5 h at 50 mA, stained with ethidium bromide (0.7 μg/ml), and photographed under UV transillumination. The extent of DNA cleavage was quantified with the Molecular Analyst software ImageJ (http://rsbweb.nih.gov/ij). The quinolone concentrations required to induce 25% of the maximum DNA cleavage (CC_{25}s) were determined for the eight FQs.

RESULTS

Expression and purification of recombinant gyrase A and B proteins. The WT *gyrA* and *gyrB* genes were amplified from *M. tuberculosis* H37Rv (1, 2, 34). The full-length *gyrA* and *gyrB* genes were inserted downstream of the T7 promoter in expression vectors pET-20b (+) and pET19b, respectively, for expression as His-tagged recombinant proteins since the His tag has been previously shown not to interfere with the catalytic functions of GyrA and GyrB (14). Resulting plasmids pTB-A (*gyrA* in pET-20b) and pTB-B (*gyrB* in pET-19b) were used to transform *E. coli* Rosetta-gami 2 (DE3)/pLysS and BL21(DE3)/pLysS, respectively. Expression of the WT *gyrA* and *gyrB* genes in *E. coli* strains by induction with IPTG and subsequent purification of the corresponding proteins by Ni-nitrilotriacetic acid affinity purification resulted in 2 and 5 mg of soluble His-tagged 93-kDa and 79-kDa proteins from 200-ml cultures, respectively. We used mutagenesis of WT *gyrB* to introduce the desired amino acid substitution and purified the corresponding GyrB-E540V protein by the same procedure as that used for WT GyrB. All recombinant subunits were obtained at high purity (>95%) in milligram amounts (see Fig. S2 in the supplemental material) and free of contaminating *E. coli* topoisomerase activity, as assessed by the lack of supercoiling activity of either GyrA or GyrB alone (Fig. 2, lanes 4 and 5).

DNA supercoiling activity of WT and GyrB-E540V DNA gyrases. Combinations of the WT GyrA and GyrB subunits were examined for DNA supercoiling activity with relaxed pBR322 DNA as the substrate in the presence and absence of ATP (Fig. 2). A combination of GyrA and GyrB at 3 μM each was sufficient for the conversion of 100% of 0.3 μg of relaxed plasmid pBR322 DNA to its supercoiled form and was used for all DNA supercoiling experiments. Since the combination of the GyrA and GyrB subunits at 3 μM led to plasmid supercoiling in the presence of ATP, reconstituted DNA gyrase was considered functional (Fig. 2, lane 3). Neither subunit alone exhibited DNA supercoiling activity in the presence of 1 mM ATP (Fig. 2, lanes 4 and 5), and no supercoiling activity was observed when ATP was absent from the reaction mixture (Fig. 2, lane 6), indicating that both subunits and ATP were essential for DNA supercoiling activity. The activity of a GyrB-E540V enzyme (designated GyrB-E540V) was also determined by DNA supercoiling assay in the presence of complementary WT GyrA (see Fig. S3 in the supplemental material).

Determination of IC_{50}s of quinolones. The inhibitory effects of quinolones on the WT and GyrB-E540V enzymes were elucidated by quinolone-inhibited DNA supercoiling assay. A set of representative data showing the inhibitory effect of CIP is shown in Fig. 3, and data for the other FQs are presented in Fig. S4 in the supplemental material. Each of the quinolones showed dose-dependent inhibition of the WT and GyrB-E540V enzymes. Inhibitory effects of quinolones against recombinant gyrases are presented as IC_{50}s ordered from low to high in Table 2. The gyrase bearing the E540V amino acid substitution in GyrB was highly resistant to inhibition by quin-

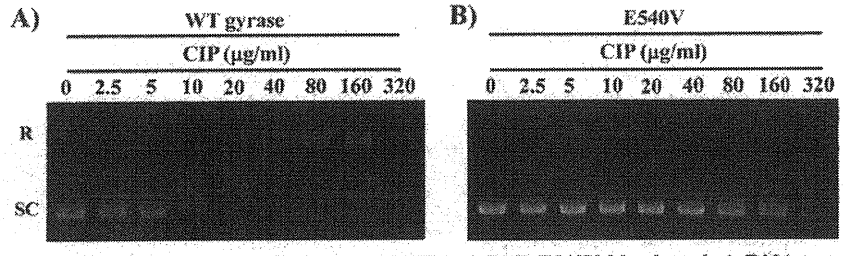

FIG. 3. Inhibitory activities of CIP on the supercoiling activities of WT and GyrB-E540V *M. tuberculosis* DNA gyrases. Relaxed pBR322 DNA (0.3 μg) was incubated with WT (A) or GyrB-E540V (B) DNA gyrase in the presence of the concentrations of CIP indicated. The reactions were stopped, and the DNA products were analyzed by electrophoresis in 1% agarose gels. R and SC denote relaxed and supercoiled pBR322 DNA, respectively.

TABLE 2. IC_{50}s and CC_{25} of FQs against WT and mutant DNA gyrases[a]

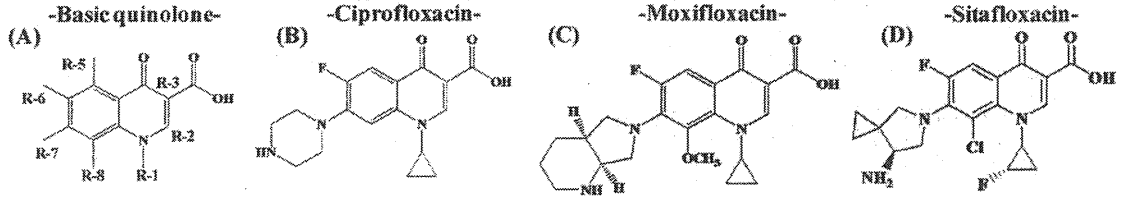

Quinolone	Substituent			IC_{50} (μg/ml)			CC_{25} (μg/ml)		
	R-1	R-7	R-8	WT	E540V	Ratio	WT	E540V	Ratio
SIX	Fluorinated cyclopropyl	Pyrrolidine	Cl	4	10	2.5	2	3	1.5
GAT	Cyclopropyl	Piperazine	O-CH_3	9	37	4.1	7	26	3.7
SPX	Cyclopropyl	Piperazine	F	7	52	7.4	10	37	3.7
MXF	Cyclopropyl	Azabicyclo	O-CH_3	16	61	3.8	5	17	3.4
LVX	Bridge N1-C8	Piperazine	Bridge N1-C8	22	82	3.7	25	57	2.3
CIP	Cyclopropyl	Piperazine	H	7	251	35.9	23	317	13.8
NOR	Ethyl	Piperazine	H	102	274	2.7	NO[b]	NO	NO
ENX	Ethyl	Piperazine	N	84	>320	>3.8	NO	NO	NO

[a] The structures of the compounds used (A, basic quinolone; B, CIP; C, MXF; D, SIX) and the locations of the substituents are shown at the top.
[b] NO, not observed.

olones (Fig. 3; Table 2; see Fig. S4 in the supplemental material). The IC_{50} of SIX was 10 μg/ml, those of GAT, LVX, MXF, and SPX were 37 to 82 μg/ml, and those of CIP, NOR, and ENX were 251, 274, and >320 μg/ml, respectively.

Quinolone-mediated DNA cleavage complex formation by WT and GyrB-E540V DNA gyrase. To examine the effects of FQs on cleavage complex formation by WT and GyrB-E540V DNA gyrase, cleavage assays were performed in which supercoiled pBR322 was incubated with WT or GyrB-E540V DNA gyrase in the presence or absence of increasing concentrations of quinolones. Figure 4 shows the results of a representative cleavage assay using CIP. Table 2 presents the CC_{25}s of the other FQs. The CC_{25}s of FQs for WT gyrase ranged from 2 to 25 μg/ml, while those for the GyrB-E540V enzyme ranged from 3 to 317 μg/ml (Table 2).

DISCUSSION

In light of the increased demand for a new treatment regimen for MDR TB, FQs have started to be used as anti-TB agents (13, 20). Although the main target of FQs is known to be bacterial DNA gyrase, the molecular details of quinolone-gyrase interactions are not yet fully understood. In this study, we examined the E540V amino acid substitution we recently found in a clinical isolate from Bangladesh (unpublished data). The same amino acid substitution has also been reported in a clinical isolate from Vietnam (12). Even though the E540 residue of GyrB, equivalent to the E466 residue in *E. coli*, has been suggested to be located in the QRDR in *M. tuberculosis* by X-ray crystallography (28), there was no experimental confirmation of this. We examined the effect of the amino acid substitution on FQ resistance at the molecular level by using purified recombinant gyrase subunits. Supercoiling and cleavage assays in the presence of several FQs demonstrated the significant contribution of the E540V amino acid substitution to quinolone resistance (Fig. 2 and 3; Table 2; see Fig. S3 and S4 in the supplemental material). These results support the model proposed by Piton et al. (28).

The structure-activity relationship between FQs and WT and GyrB-E540V gyrases were analyzed. All eight FQs studied have a substituent, pyrrolidine, piperazine, or azabicyclo, at R-7 which has been suggested to be associated with E540 on GyrB (28). NOR and ENX, with an ethyl residue at R-1, have high IC_{50}s (102 and 84 μg/ml, respectively), whereas the other FQs, with a cyclopropyl at R-1 or an N1-C8 bridge, have significantly lower IC_{50}s (4 to 22 μg/ml) for WT gyrase, suggesting that a cyclopropyl at R-1 or an N1-C8 bridge contributes to FQ activity. Although higher IC_{50}s of all FQs were observed for the GyrB-E540V enzyme than for the WT en-

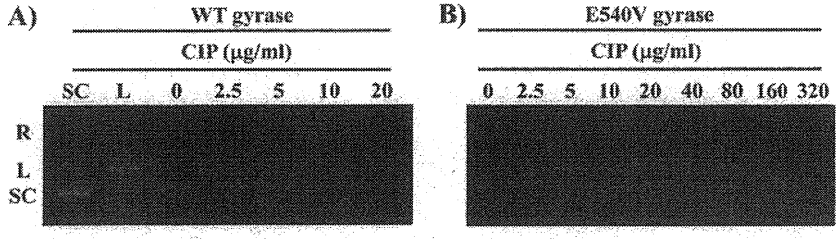

FIG. 4. CIP-mediated DNA cleavage complex by WT and GyrB-E540V gyrases of *M. tuberculosis*. Supercoiled pBR322 DNA (0.3 μg) was incubated with WT (A) or GyrB-E540V (B) DNA gyrase in the presence of the concentrations of CIP indicated. After addition of SDS and protease K, the reactions were stopped and the mixture samples were analyzed by electrophoresis in 0.8% agarose gels. R, L, and SC denote relaxed, BamHI-linearized, and supercoiled pBR322 DNA, respectively.

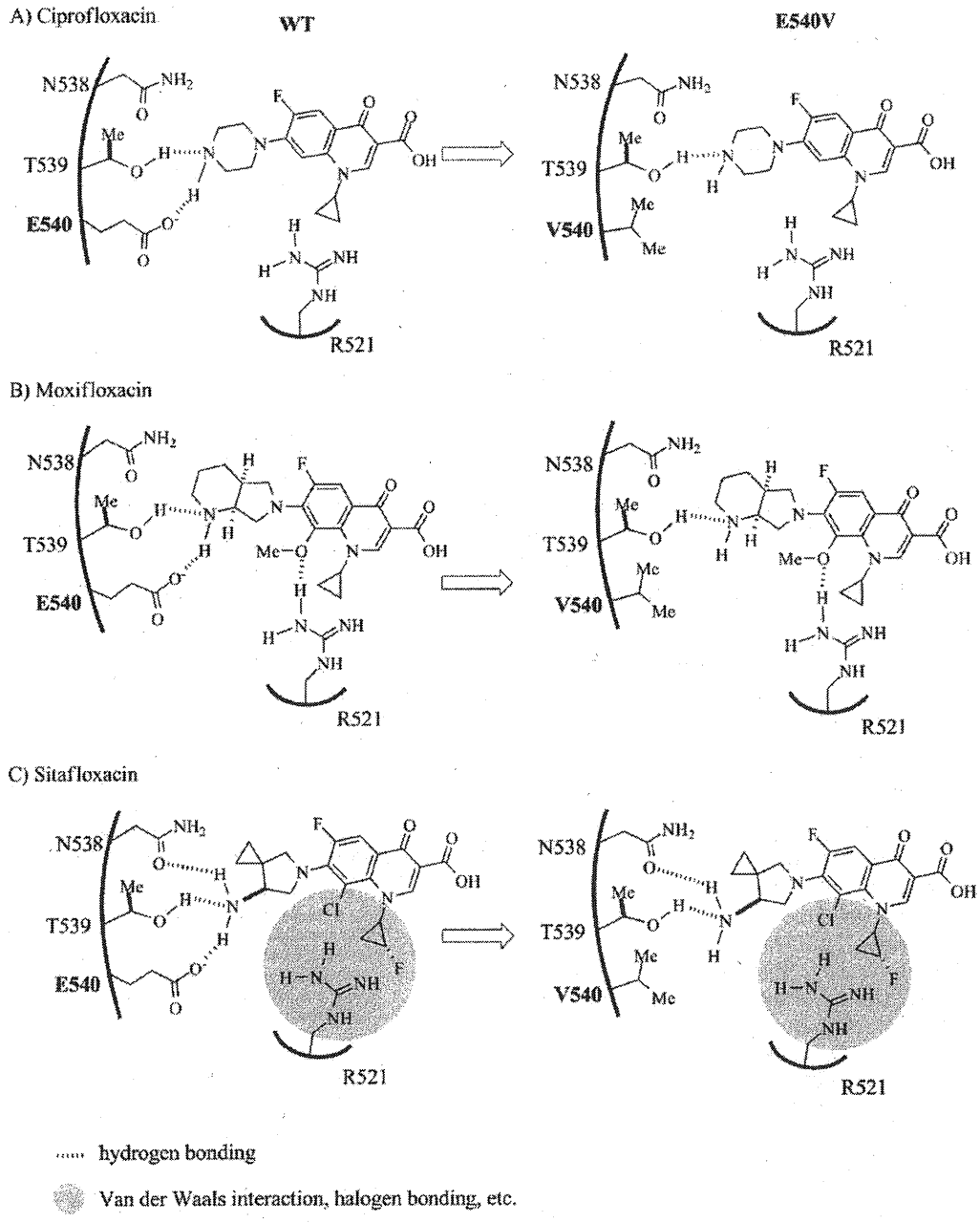

FIG. 5. Hypothetical models of interactions of WT and E540V GyrB with quinolones with substituents at R-7 and R-8. The models show the hydrogen bonding network relationship between residues of the WT and E540V gyrases and the R-7 and R-8 groups of CIP (A). Panels B and C show the relationships of MXF and SIX with the QBP of the DNA GyrB subunit of *M. tuberculosis*. The left and right panels show the WT and GyrB-E540V gyrase activities for hydrogen interaction with quinolones. Position 540 is indicated by bold type.

zyme, the difference in the two IC_{50}s was lowest for SIX. In particular, this FQ has a fluorinated cyclopropyl ring at R-1 while four other FQs, GAT, SPX, MXF, and CIP, have a cyclopropyl. In contrast, the difference between the CIP IC_{50}s for the E540V and WT enzymes was significantly high. The only apparent difference between CIP and the other effective FQs was the absence of a substituent at R-8 (Table 2). We have also attempted to elucidate the effects of the E540V amino acid substitution in GyrB using DNA cleavage assays (Fig. 4 and Table 2) to confirm the results obtained by quinolone-inhibited supercoiling assays.

Amino acid residues in GyrB located close to E540 (E501 in reference 28), including N538 (N499) and T539 (T500) on the α2 helix and R482 (R521) on β2, have been proposed to interact with the GyrA subunit and DNA strands to form the QBP (28). It has been suggested that the β1-α1 loop (residues 498 to 501 in GyrB of *M. tuberculosis*) interacts with the R-1 group, the β2-DBL (DNA-binding loop, residues 519 to 525)

interacts with the R-7 and R-8 groups, and the beginning of α2 (residues 537 to 541) interacts with the R-7 group (28). A substitution of the glutamic acid at position 540 with a valine may therefore lead to a conformational change in QBP geometry in GyrB (28).

Based on the crystal structure and current data obtained with several FQs (5, 16, 28), we hypothesize the mechanism of FQ resistance conferred by the E540V amino acid substitution on GyrB as shown in Fig. 5. The hydrogen bonding network involving E540 could play a pivotal role in the recognition of quinolones by the GyrB subunit on QBP. One of the FQs, CIP, exerts potent inhibitory activity against WT DNA gyrase (IC_{50} = 7 μg/ml) and may bind tightly to GyrB through two hydrogen bonds (O-H—N and O^-—H-N) involving a hydroxyl group (OH) of the T539 residue and a carboxylate (CO_2^-) of the E540 residue (Fig. 5A, left; Table 2). In contrast, the efficacy of CIP against the GyrB-E540V gyrase is drastically lower (IC_{50} = 251 μg/ml). The E540V amino acid substitution replaces glutamic acid, which bears a carboxyl group, with valine, which is nonpolar and sterically demanding. The subsequent loss of the hydrogen bonding interactions with E540 could induce a substantial conformational change, which would disrupt binding with CIP (Fig. 5A, right). The efficacy of other FQs carrying a substituent at R-8 against the E540V enzyme was shown to be higher than that of CIP (Table 2). For example, MXF showed inhibitory activities against WT GyrB and E540V GyrB, with IC_{50}s of 16 and 61 μg/ml, respectively. MXF and CIP vary structurally with regard to the substituents at R-7 and R-8: MXF has a bulky azabicyclo group at R-7 and a methoxy group at R-8, whereas CIP has a simple piperazine group at R-7 and no substituent at R-8 (Table 2). In the binding of MXF with WT GyrB (Fig. 5B, left), the substituents at R-7 and R-8 may efficiently interact with residues of the GyrB subunit through three hydrogen bonding networks involving T539 (O-H—N), E540 (O^-—H-N), and R521 (H-N-H—O-Me). With regard to the GyrB E540V gyrase (Fig. 5B, right), however, MXF could still retain a substantial affinity for the GyrB subunit through hydrogen bonding with the substituents at R-7 and R-8 (O-H—N and H-N-H—O-Me), whereas CIP could not retain such an affinity due to the absence of hydrogen bonding with the substituent at R-8 and would thus be more sensitive to the amino acid substitution. Apart from MXF and CIP, SIX carries a pyrrolidine at R-7 and a halide (chlorine) at R-8 and exhibits potent activities toward the WT (IC_{50} = 4 μg/ml) and GyrB-E540V (IC_{50} = 10 μg/ml) gyrase enzymes. As shown in Fig. 5C, the substituents at R-7 and R-8 of SIX may interact with the residues of the WT GyrB subunit through three hydrogen bonds and van der Waals forces and/or halogen bonding (4) involving T539 (O-H—N), E540 (O^-—H-N), N538 (O-O—H-N), and R521 (van der Waals radius zone between residue R521 and the R-8 halide group). It seems likely that interactions between R521 and the substituents at R-1 and R-8 are sufficient to make up for the loss of hydrogen bonding with the GyrB-E540V gyrase and thus play important roles in the binding of SIX.

In summary, our study indicates that the E540V amino acid substitution in GyrB is involved in the resistance of *M. tuberculosis* against quinolones, although E540 is reported to be outside GyrB QRDRs. We thus propose that the E540 residue be included in the QRDR in *M. tuberculosis* as shown in *Streptococcus pneumoniae* (23, 26). Moreover, we also demonstrated an association between structural features of quinolones and activities against the WT and E540V forms of the GyrB DNA gyrase subunit of *M. tuberculosis*. The interaction between FQs and GyrB, which is composed of hydrogen bonding networks involving substituents of FQs and amino acid residues of QBP in GyrB, plays an important role in the inhibitory activity of FQs. Further studies investigating the contributions of other amino acid substitutions may also help gain a comprehensive understanding of the mechanism by which FQ-resistant TB emerges.

ACKNOWLEDGMENTS

We thank Haruka Suzuki, Yukari Fukushima, and Aiko Ohnuma for their technical support with several of the experiments and Yusuke Suzuki and Kyeong Hwa Bae for their helpful comments.

This work was supported by a grant from U.S.-Japan Cooperative Medical Science Programs, the Global Center of Excellence (COE) Program, Establishment of International Collaboration Centers for Zoonosis Control, Ministry of Education, Culture, Sports, Science, and Technology (MEXT), Japan, in part by J-GRID, the Japan Initiative for Global Research Network on Infectious Diseases from MEXT to Y.S., and by Grants-in-Aid for Scientific Research from the Japan Society for the Promotion of Science (JSPS) to Y.S. and C.N.

REFERENCES

1. **Aubry, A., X. S. Pan, L. M. Fisher, V. Jarlier, and E. Cambau.** 2004. *Mycobacterium tuberculosis* DNA gyrase: interaction with quinolones and correlation with antimycobacterial drug activity. Antimicrob. Agents Chemother. **48:**1281–1288.
2. **Aubry, A., et al.** 2006. Novel gyrase mutations in quinolone-resistant and -hypersusceptible clinical isolates of *Mycobacterium tuberculosis*: functional analysis of mutant enzymes. Antimicrob. Agents Chemother. **50:**104–112.
3. **Aziz, M. A., et al.** 2006. Epidemiology of antituberculosis drug resistance (the Global Project on Anti-tuberculosis Drug Resistance Surveillance): an updated analysis. Lancet **368:**2142–2154.
4. **Barnard, F. M., and A. Maxwell.** 2001. Interaction between DNA gyrase and quinolones: effects of alanine mutations at GyrA subunit residues Ser^{83} and Asp^{87}. Antimicrob. Agents Chemother. **45:**1994–2000.
5. **Bax, B. D., et al.** 2010. Type IIA topoisomerase inhibition by a new class of antibacterial agents. Nature **466:**935–940.
6. **Blumberg, H. M., et al.** 2003. American Thoracic Society/Centers for Disease Control and Prevention/Infectious Diseases Society of America: treatment of tuberculosis. Am. J. Respir. Crit. Care Med. **167:**603–662.
7. **Champoux, J. J.** 2001. DNA topoisomerases: structure, function, and mechanism. Annu. Rev. Biochem. **70:**369–413.
8. **Cole, S. T., et al.** 1998. Deciphering the biology of *Mycobacterium tuberculosis* from the complete genome sequence. Nature **393:**537–544.
9. **Corbett, K. D., and J. M. Berger.** 2004. Structure, molecular mechanisms, and evolutionary relationships in DNA topoisomerases. Annu. Rev. Biophys. Biomol. Struct. **33:**95–118.
10. **Drlica, K.** 1999. Mechanisms of fluoroquinolone action. Curr. Opin. Microbiol. **2:**504–508.
11. **Drlica, K., and X. Zhao.** 1997. DNA gyrase, topoisomerase IV, and the 4-quinolones. Microbiol. Mol. Biol. Rev. **61:**377–392.
12. **Duong, D. A., et al.** 2009. Beijing genotype of *Mycobacterium tuberculosis* is significantly associated with high-level fluoroquinolone resistance in Vietnam. Antimicrob. Agents Chemother. **53:**4835–4839.
13. **Fattorini, L., et al.** 1999. Activity of 16 antimicrobial agents against drug-resistant strains of *Mycobacterium tuberculosis*. Microb. Drug Resist. **5:**265–270.
14. **Freydank, A. C., W. Brandt, and B. Dräger.** 2008. Protein structure modeling indicates hexahistidine-tag interference with enzyme activity. Proteins **72:**173–183.
15. **Frieden, T. R., et al.** 1993. The emergence of drug-resistant tuberculosis in New York City. N. Engl. J. Med. **328:**521–526.
16. **Fu, G. S., et al.** 2009. Crystal structure of DNA gyrase B′ domain sheds lights on the mechanism for T-segment navigation. Nucleic Acids Res. **37:**5908–5916.
17. **Gillespie, S. H., and N. Kennedy.** 1998. Fluoroquinolones: a new treatment for tuberculosis? Int. J. Tuberc. Lung Dis. **2:**265–271.
18. **Gore, J., et al.** 2006. Mechanochemical analysis of DNA gyrase using rotor bead tracking. Nature **439:**100–104.
19. **Guillemin, I., V. Jarlier, and E. Cambau.** 1998. Correlation between quinolone susceptibility patterns and sequences in the A and B subunits of DNA gyrase in mycobacteria. Antimicrob. Agents Chemother. **42:**2084–2088.

20. **Hatfull, G. F., and W. R. Jacobs, Jr.** 2000. Molecular genetics of mycobacteria, p. 235–256. American Society for Microbiology, Washington, DC.
21. **Heeb, S., et al.** 2011. Quinolones: from antibiotics to autoinducers. FEMS Microbiol. Rev. **35:**247–274.
22. **Infectious Diseases Society of the Republic of China; Society of Tuberculosis, Taiwan; Medical Foundation in Memory of Deh-Lin Cheng; Foundation of Wei-Chuan Hsieh for Infectious Diseases Research and Education; C Y Lee's Research Foundation for Pediatric Infectious Diseases and Vaccines.** 2004. Guidelines for chemotherapy of tuberculosis in Taiwan. J. Microbiol. Immunol. Infect. **37:**382–384.
23. **Laponogov, I., et al.** 2010. Structural basis of gate-DNA breakage and resealing by type II topoisomerases. PLoS One **5:**e11338.
24. **Levine, C., H. Hiasa, and K. J. Marians.** 1998. DNA gyrase and topoisomerase IV: biochemical activities, physiological roles during chromosome replication, and drug sensitivities. Biochim. Biophys. Acta **1400:**29–43.
25. **Pan, X. S., G. Yague, and L. M. Fisher.** 2001. Quinolone resistance mutations in *Streptococcus pneumoniae* GyrA and ParC proteins: mechanistic insights into quinolone action from enzymatic analysis, intracellular levels, and phenotypes of wild-type and mutant proteins. Antimicrob. Agents Chemother. **45:**3140–3147.
26. **Pan, X. S., K. A. Gould, and L. M. Fisher.** 2009. Probing the differential interactions of quinazolinedione PD 0305970 and quinolones with gyrase and topoisomerase IV. Antimicrob. Agents Chemother. **53:**3822–3831.
27. **Pitaksajjakul, P., et al.** 2005. Mutations in the *gyrA* and *gyrB* genes of fluoroquinolone-resistant *Mycobacterium tuberculosis* from TB patients in Thailand. Southeast Asian J. Trop. Med. Public Health **36**(Suppl. 4)**:**228–237.
28. **Piton, J., et al.** 2010. Structural insights into the quinolone resistance mechanism of *Mycobacterium tuberculosis* DNA gyrase. PLoS One **5:**e12245.
29. **Reece, R. J., and A. Maxwell.** 1991. DNA gyrase: structure and function. Crit. Rev. Biochem. Mol. Biol. **26:**335–375.
30. **Sepkowitz, K. A., E. E. Telzak, S. Recalde, and D. Armstrong.** 1994. Trend in the susceptibility of tuberculosis in New York City, 1987-1991. Clin. Infect. Dis. **18:**755–759.
31. **Sharma, S. K., and A. Mohan.** 2004. Multidrug-resistant tuberculosis. Indian J. Med. Res. **120:**354–376.
32. **Sun, Z., et al.** 2008. Comparison of *gyrA* gene mutations between laboratory-selected ofloxacin-resistant *Mycobacterium tuberculosis* strains and clinical isolates. Int. J. Antimicrob. Agents **31:**115–121.
33. **Takiff, H. E., et al.** 1994. Cloning and nucleotide sequence of *Mycobacterium tuberculosis gyrA* and *gyrB* genes and detection of quinolone resistance mutations. Antimicrob. Agents Chemother. **38:**773–780.
34. **Veziris, N., et al.** 2007. Treatment failure in a case of extensively drug-resistant tuberculosis associated with selection of a GyrB mutant causing fluoroquinolone resistance. Eur. J. Clin. Microbiol. Infect. Dis. **26:**423–425.
35. **World Health Organization.** 2010. Multidrug and extensively drug-resistant TB (M/XDR-TB). Global report on surveillance and response. Document WHO/HTM/TB/2010.3. World Health Organization. Geneva, Switzerland.
36. **World Health Organization.** 2010. Global tuberculosis control: WHO report. Document WHO/HTM /TB/2010.7. World Health Organization, Geneva, Switzerland.
37. **World Health Organization.** 2008. Guidelines for the programmatic management of drug-resistant tuberculosis. WHO/HTM/TB/2008.402. World Health Organization, Geneva, Switzerland.
38. **World Health Organization.** 2008. Anti-tuberculosis drug resistance in the world fourth global report. The WHO/IUATLD Global Project on Anti-tuberculosis Drug Resistance Surveillance 2002-2007 WHO/HTM/TB/2008.394. World Health Organization, Geneva, Switzerland.
39. **Zhou, J., et al.** 2000. Selection of antibiotic-resistant bacterial mutants: allelic diversity among fluoroquinolone-resistant mutations. J. Infect. Dis. **182:**517–525.
40. **Zignol, M., et al.** 2006. Global incidence of multidrug-resistant tuberculosis. J. Infect. Dis. **194:**479–485.

Rapid detection of *Mycobacterium tuberculosis* complex in cattle and lechwe (*Kobus leche kafuensis*) at the slaughter house

Mudenda B. Hang'ombe,[1] Chie Nakajima,[2] Akihiro Ishii,[2] Yukari Fukushima,[2] Musso Munyeme,[1] Wigganson Matandiko,[3] Aaron S. Mweene,[1] Yasuhiko Suzuki[2,4]

[1]School of Veterinary Medicine, University of Zambia, Lusaka, Zambia; [2]Hokkaido University Research Center for Zoonosis Control, Sapporo, Hokkaido, Japan; [3]Zambia Wildlife Authority, Private Bag 001, Chilanga, Zambia; [4]JST/JICA-SATREPS

Abstract

The detection and diagnosis of tuberculosis (TB) in food-producing animals is critical to human health. In this study we applied the loop-mediated isothermal amplification (LAMP) system to detect *Mycobacterium tuberculosis* complex (MTC) directly in 57 cattle and six lechwe (*Kobus leche kafuensis*) carcasses exhibiting lesions characteristic of TB. The samples were first subjected to Ziehl-Neelsen microscopy, followed by culture and LAMP assay. In addition, multiplex-PCR was used to determine the species involved. Of the samples from the cattle, 84.2% (95% confidence interval: 71.6-92.1) were found positive with Ziehl-Neelsen microscopy, 93.0% (95% confidence interval: 82.2-97.7) with culture, and 94.7% (95% confidence interval: 84.5-98.6) with the LAMP system while the *Kobus leche kafuensis* samples were all positive for all techniques used. These results indicate that the LAMP system can be used to augment the detection and surveillance of TB in animals; hence can be a very useful tool in the veterinary field and in public health.

Introduction

The detection and diagnosis of tuberculosis (TB) in animals involves clinical examination, tuberculin skin tests, and the gamma interferon immunoassay.[1,2] Other techniques involve detection on meat inspection or postmortem followed by the usual course of microscopic observation of acid-fast bacilli, bacterial cultures, and molecular confirmation methods.[3] TB in animals can be caused by *Mycobacterial* species belonging to the *Mycobacterium tuberculosis* complex (MTC). This group comprises several closely related species responsible for strictly human and zoonotic TB. These include *M. tuberculosis, M. africanum, M. microti, M. bovis, M. caprae*, and *M. pinnipedii*.[4-6] Some of these *Mycobacterium* species are major re-emerging zoonotic agents of bovine TB, the prevalence of which depends on direct exposure to cattle and consumption of unpasteurized dairy products.[7,8] Furthermore, the interaction in the human-livestock-wildlife interphase areas of some wildlife animals like lechwe (*Kobus leche kafuensis*), documented with *M. bovis*, have broadened the reservoir base for MTC.[9]

In this regard, detection and diagnosis of TB is very important as a way of mitigating its spread in the human population. Currently, a novel molecular amplification method termed the loop-mediated isothermal amplification system (LAMP) has been developed.[10] The system shows a high amplification efficiency and has been used to diagnose several other diseases.[10-17] The objective of our study was to evaluate the applicability of the LAMP system, in the veterinary field, to detect MTC directly from suspected TB lesions of cattle and wildlife being slaughtered for food.

Materials and Methods

Sampling

Our study was conducted on samples collected from the slaughtered animals along the examination line. The animals were examined for gross lesions according to the standard postmortem procedures as described previously.[18] Organs and tissues with suspected TB lesions were collected after detailed postmortem examination of the entire carcasses. Following collection, the specimens were placed into a cooler box with ice packs before transportation to the laboratory for analysis.

Preparation of samples for evaluation

To prepare the suspected TB samples for analysis, the suspected tissues with lesions were trimmed of fat and then a 500-mg sample was collected. The sample was then minced with sterile scissors and homogenized in a sterilized glass homogenizer, after which 1 mL of phosphate buffer (pH 6.8) was added. After thorough mixing, 1 mL of 5% sodium hydroxide was added. This was mixed thoroughly and then incubated for 15 min at room temperature. To this mixture 10 mL of phosphate buffer was added and then centrifuged at 1500 *g* for 20 min. The pellet was collected and then resuspended in a final volume of 0.5 mL of phosphate buffer. This was used for inoculation into 2% Ogawa medium and preparation of slides for Ziehl-Neelsen (ZN) microscopy. Cultures were monitored for growth up to 8 wk at 37°C. Another 100 µL of the suspension was used to prepare DNA directly by using DNAzol reagent (Invitrogen, Carlsbad, CA, USA). The suspension was mixed with 1.0 mL of DNAzol reagent and mechanical disruption was used as previously described.[19] DNA was extracted according to the manufacturer's instructions. Genomic DNA from *Mycobacterium* bacterial cultures was also prepared from colonies using DNAzol and mechanical disruption as described earlier. The extracted DNA was then dissolved in 50 µL TE buffer consisting of 10 mM Tris/HCL (pH 8.0) and 1 mM EDTA.

Correspondence: Mudenda Bernard Hang'ombe, School of Veterinary Medicine, Department of Paraclinical Studies, P. O. Box 32379, Lusaka, Zambia.
E-mail: mudenda68@yahoo.com

Key words: *Mycobacterium bovis*, cattle, *Kobus leche kafuensis*, LAMP, multiplex-PCR.

Acknowledgments: the authors are grateful to Mr L. Moonga and Mr E. Mulenga from the Department of Paraclinical Studies, School of Veterinary Medicine, University of Zambia for their technical assistance. This work was supported by the Directorate of Research and Graduate Studies of the University of Zambia, the Ministry of Education, Culture, Sports, Science and Technology of Japan (MEXT), and the Global Center of Excellence (COE) program for the Establishment of International Collaboration Centers for Zoonoses control, by grants from the US-Japan Cooperative Medical Science program to YS and the Japan Society for the Promotion of Science to YS and CH.

Contributions: MBH, sample collection, isolation, LAMP and PCR detection, analysis, data interpretation, and manuscript drafting; CN, AI, YF, MM, WM, design of study, sample collection, and manuscript drafting; ASM, YS, interpretation of data, drafting, and final approval of manuscript.

Conflict of interest: the authors report no conflicts of interest.

Received for publication: 3 March 2011.
Accepted for publication: 29 April 2011.

Veterinary Science Development 2011; 1:e5
doi:10.4081/vsd.2011.e5

LAMP

LAMP reactions were performed in a total volume of 25 μL consisting of 30 pmol each of inner primers FIP and BIP, 5 pmol each of outer primers F3 and B3, 20 pmol each of loop primers FLP and BLP, 1.4 mM deoxynucleotide triphosphate, 0.8 M betaine, 20 mM Tris/HCl (pH 8.8), 10 mM KCl, 10 Mm $(NH4)_2SO_4$, 8 mM $MgSO_4$ and 8 U Bst DNA polymerase (New England Biolabs, USA) with 2 μL sample DNA. The sequences of the primers used are shown in Table 1.

The primers used in our study have also been used by other workers to detect MTC in human sputum samples.[17] The mixture was then incubated at 64°C for 1 hr in a thermal dry heat block (ALB 221; Iwaki, Tokyo, Japan). A negative control (buffer) and positive control were included in each run. Results were visualized with the fluorescence detection reagent (Eiken Chemical Co., Tochigi, Japan) according to the manufacturer's instructions.

Multiplex-PCR primers and conditions

Genomic DNA from *Mycobacterium* bacterial cultures was used as a template. Primer pairs for *cfp32* (a specific gene for MTC), RD9 (region of difference 9 seen only in *M. tuberculosis* and *M. canettii*), and RD12 (region of difference 12 deleted in *M. bovis, M. caprae*, and *M. canettii*) were obtained from an earlier publication.[20] The general PCR recipe contained 7.4 μL H_2O, 2 μL 10 x Taq buffer, 2 μL dNTPs (2.5 mM each), 0.2 μL Taq (Takara), 1 μL target DNA, 2.2 μL of 10 μM *cfp32* primers, 0.7 μL of 5 μM RD9 primers, and 0.8 μL of 5 μM RD12 primers. Appropriate negative controls consisting of PCR mix without target DNA were included. The PCR was performed using the following program: denaturation for 1 min at 98°C followed by 35 cycles of 5 sec at 98°C, 20 sec at 58°C, and 1 min at 68°C with final extension for 5 min at 72°C in a thermalcycler (iCycler, Bio-Rad Laboratories Inc., CA, USA). All PCR products were identified by gel electrophoresis in a 2.0% agarose gel and were visualized by ethidium bromide staining.

Results

A total of 388 carcasses were examined, comprising 358 cattle and 30 lechwe. Of these animals examined, 57 (15.9% CI: 12.4-20.2) cattle carcasses had lesions characteristic of TB in the tissues and organs while 6 (20% CI: 8.40-39.1) lechwe carcasses had such lesion exhibitions as well. When these samples were subjected to ZN microscopy, 48 (84.2% CI: 71.6-92.1) and 6 (100% CI: 51.7-100) samples from the cattle and lechwe, respectively, were found positive. In the case of the cattle, 9 samples were found to be negative, from those observed with characteristic TB lesions. On culture of postmortem TB-positive samples, 53 (93.0% CI: 82.2-97.7) cattle and all lechwe observed at meat inspection were found to be positive for acid-fast bacilli. The positive sample specimens increased in number with the LAMP system. Furthermore, the positive reactions on LAMP were easy to determine with the naked eye, as shown in Figure 1.

Table 1. Primers for the specific detection of the *Mycobacterium tuberculosis* complex used in the study.

Name of primer	Sequence
FIP	CACCCACGTGTTACTCATGCAAGTCGAACGGAAAGGTCT
BIP	TCGGGATAAGCCTGGACCACAAGACATGCATCCCGT
F3	CTGGCTCAGGACGAACG
B3	GCTCATCCCACACCGC
FLP	GTTCGCCACTCGAGTATCTCCG
BLP	GAAACTGGGTCTAATACCGG

Table 2. Number and percentage of samples testing positive for *Mycobacterium tuberculosis* under different procedures.

Sample source	Ziehl-Neelsen microscopy	Culture	LAMP
Cattle	48 (84.2%)	53 (93.0%)	54 (94.7%)
Lechwe	6 (100%)	6 (100%)	6 (100%)
Total	54	59	60
Sensitivity	85.7%	93.7%	95.2%
95% CI	74.1-92.9	83.7-97.9	85.8-98.8

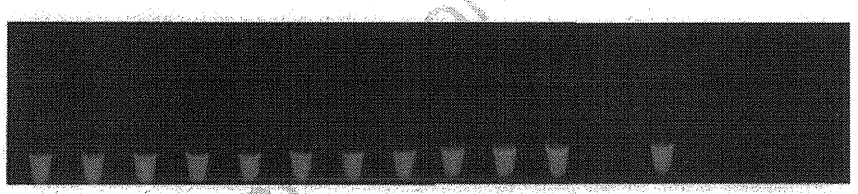

Figure 1. Visual detection of LAMP products under the UV light. From left to right, tubes12, 14, 15, and 16 are negative, while the rest are positive.

The overall results for the detection of TB-positive samples are shown in Table 2. All of the culture positive samples were positive on the LAMP assay. The culture isolates were also subjected to the LAMP system and were found to be MTC. In terms of sensitivity, the LAMP system was 100% positive in culture positive specimens. An additional sample not detected with culture was also found to be positive. The sensitivity of ZN microscopy was found to be 85.7%, while culture was 93.7%, and LAMP 95.2%, respectively. In all these diagnostic procedures, sensitivity was taken as the proportion of samples testing positive for *Mycobacterium* tuberculosis.

The multiplex-PCR was successfully used to identify the MTC species involved in cattle and lechwe. The amplicon of 786bp of the *cfp32* region was observed as indicated in Figure 2, showing that the MTC species involved in these cases was *M. bovis*. All of the cultures were positive for this amplicon indicating the MTC strain in the domestic and wildlife animals to be *M. bovis*.

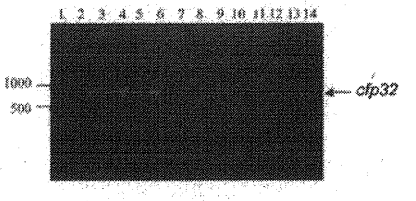

Figure 2. Multiplex-PCR products analyzed with 2% agarose gel electrophoresis followed by ethidium bromide staining. Lane 1 is a 50 bp ladder and lane 13 is a negative control.

Discussion

We successfully applied the LAMP assay technique for the rapid detection of the MTC group directly from clinical samples. It is important to note that the diagnosis of TB in

animals largely depends on the tuberculin skin testing and slaughterhouse surveillance for undetected infections.[1] In addition, it would be useful to develop a rapid and sensitive method to apply to doubtful TB-suspected samples. Slaughterhouse surveillance of TB is one of the key tools for detecting and confirming suspected TB cases. This is aided by microscopic analysis of sample smears, which is a rapid method of detecting acid-fast bacilli.[3] However, this method is limited in sensitivity and the ability to identify infecting species. The culture method can be used efficiently to diagnose TB, but it is time consuming as it requires a minimum of four weeks. Therefore, a test that combines the rapidity of microscopy and sensitivity of bacterial culture methods would facilitate easy diagnosis at slaughter houses and establishments requiring definite results at the shortest possible time. The test can be a valuable tool in veterinary diagnostics. In our study, there was efficient amplification of the LAMP system to detect MTC from suspected specimens from cattle and lechwe. These results clearly demonstrate the high sensitivity of the LAMP system in detecting TB as observed by others who have been working on human specimens.[11,17,21] This result also suggests that LAMP may be superior to all procedures being used at the moment to detect TB in animals. One sample was detected as positive on LAMP although negative on culture. This could be attributed to low numbers of MTC viable cells in the section of the specimen under investigation. *M. bovis* was identified from the results of the multiplex-PCR, which targets three genetic regions that are *cfp32*, RD9 and RD12.[6,22-24]

In summary, our study clearly provides evidence that the LAMP assay is a method that allows direct detection of MTC from processed clinical/abattoir specimens. This means that the technique can also be applied in the field of veterinary medicine for rapid confirmation of suspected cases. The ease of use and high sensitivity of this assay may facilitate the diagnosis and confirmation of MTC at slaughter houses, hence improving surveillance and control of TB at herd levels and in veterinary medicine in general.

References

1. de la Rua-Domenech R, Goodchild AT, Vordermeier HM, et al. Ante mortem diagnosis of tuberculosis in cattle: a review of the tuberculin tests, gamma-interferon assay and other ancillary diagnostic techniques. Res Vet Sci 2006;81:190-210.
2. Schiller I, Vordermeier HM, Waters WR, et al. Comparison of tuberculin activity using the interferon-gamma assay for the diagnosis of bovine tuberculosis. Vet Rec 2010;167:322-36.
3. Kent BD, Kubica GP. Public Health Mycobacteriology: a Guide for the Level III Laboratory. Atlanta: U.S. Department of Health and Human services, Centers for Disease Control, 1985.
4. Aranaz A, Cousins D, Mateos A, Dominquez, L. Elevation of Mycobacterium tuberculosis subsp. caprae Aranaz et al. 1999 to species rank as Mycobacterium caprae comb. Nov., sp. Nov. Int J Syst Evol Micr 2003;53:1785-9.
5. Cousins DV, Bastida R, Cataldi A, et al. Tuberculosis in seals caused by a novel member of the Mycobacterium tuberculosis complex: Mycobacterium pinnipedii sp. Nov. Int J Syst Evol Micr 2003;53:1305-14.
6. Huard RC, Fabre M, Haas PD, et al. Novel genetic polymorphisms that further delineate the phylogeny of the Mycobacterium tuberculosis complex. J Bacteriol 2006;188:4271-87.
7. Cosivi O, Grange JM, Daborn CJ, et al. Zoonotic tuberculosis due to Mycobacterium bovis in developing countries. Emerg Infect Dis 1998;4:59-70.
8. Michel AL. Implications of tuberculosis in African wildlife and livestock. Ann NY Acad Sci 2002;969:251-5.
9. Pandey GS. Studies of the infectious diseases of the Kafue lechwe (Kobus lechwe kafuensis) with particular reference to tuberculosis in Zambia. PhD thesis, Azabu, University, Tokyo, Japan, 1998.
10. Notomi T, Okayama H, Masubuchi H, et al. Loop-mediated isothermal amplification of DNA. Nucleic Acids Res 2000;28:E63.
11. Iwamoto T, Sonobe T, Hayashi K. Loop-mediated isothermal amplification for direct detection of Mycobacterium tuberculosis complex, M. avium and M. intracellulare. J Clin Microbiol 2003;41:2616-22.
12. Kuboki N, Inoue N, Sakurai T, et al. Loop-mediated isothermal amplification for detection of African trypanosomes. J Clin Microbiol 2003;41:5517-24.
13. Parida M, Posadas G, Inoue GPS, Hasebe F, Morita K. Real-time reverse transcription loop-mediated isothermal amplification for rapid detection of West Nile virus. J Clin Microbiol 2004;42:257-63.
14. Parida M, Horioke K, Ishida H, et al. Rapid detection and differentiation of dengue virus serotypes by a real-time reverse transcription-loop mediated isothermal amplification assay. J Clin Microbiol 2005;43:2895-903.
15. Kimura H, Ihara M, Enomoto Y, et al. Rapid detection of herpes simplex virus DNA in cerebrospinal fluid: comparison between loop-mediated isothermal amplification and real-time PCR. Med Microbiol Immun 2005;194:181-5.
16. Yoda T, Suzuki Y, Yamazaki K, et al. Evaluation and application of reverse transcription loop-mediated isothermal amplification for detection of noroviruses. J Med Virol 2007;79:326-34.
17. Pandey BD, Poudel A, Yoda T, et al. Development of an in-house loop-mediated isothermal amplification (LAMP) assay for detection of Mycobacterium tuberculosis and evaluation in sputum samples of Nepalese patients. J Med Microbiol 2008;57:439-43.
18. Gracey JF, Collins DS, Huey J. eds. Meat Hygiene. 10th edn. Toronto: WB Saunders & Company, 1999.
19. Suzuki Y, Katsukawa C, Inoue K, et al. Mutations in rpoB gene of rifampicin resistant clinical isolates of Mycobacterium tuberculosis in Japan. Kansenshogaku Zasshi 1995;69:413-19.
20. Nakajima C, Rahim Z, Fukushima Y, et al. Identification of Mycobacterium tuberculosis clinical isolates in Bangladesh by a species distinguishable multiplex PCR. BMC Infect Dis 2010;10:118.
21. Boehme CC, Nabeta P, Henostroza G, et al. Operational feasibility of using loop mediated isothermal amplification for diagnosis of pulmonary tuberculosis in microscopy centers of developing countries. J Clin Microbiol 2007;45:1936-40.
22. Brosch R, Gordon SV, Marmiesse M, et al. A new evolutionary scenario for the Mycobacterium tuberculosis complex. Proc Natl Acad Sci USA 2002;99:3684-9.
23. Huard RC, Lazzarini LC, Butler WR, Van Soolingen D, Ho JL. PCR based method to differentiate the subspecies of the Mycobacterium tuberculosis Complex on the basis of genomic deletions. J Clin Microbiol 2003;41:1637-50.
24. Huard RC, Chitale S, Leung M, et al. The Mycobacterium tuberculosis complex restricted gene cfp32 encodes an expressed protein that is detectable in tuberculosis patients and is positively correlated with pulmonary interleukin-10. Infect Immun 2003;71:6871-83.

JOURNAL OF CLINICAL MICROBIOLOGY, Apr. 2011, p. 1354–1362 Vol. 49, No. 4
0095-1137/11/$12.00 doi:10.1128/JCM.02274-10

Genotypes and Characteristics of Clustering and Drug Susceptibility of *Mycobacterium tuberculosis* Isolates Collected in Heilongjiang Province, China▽

Juan Wang,[1]† Yan Liu,[2]† Chun-Lei Zhang,[3]† Bin-Ying Ji,[3] Liu-Zhuo Zhang,[2] Yong-Zhen Shao,[1]‡ Shui-Lian Jiang,[1] Yasuhiko Suzuki,[4] Chie Nakajima,[4] Chang-Long Fan,[3] Yuan-Ping Ma,[1] Geng-Wen Tian,[1] Toshio Hattori,[5] and Hong Ling[1]*

Department of Microbiology and Parasitology, Heilongjiang Provincial Key Laboratory for Infection and Immunity, Key Lab of Heilongjiang Province, Education Bureau for Etiology,[1] and Department of Biostatistics,[2] Harbin Medical University, Harbin, China; Harbin Chest Hospital, Harbin, China[3]; Department of Global Epidemiology, Hokkaido University, Research Center for Zoonosis Control, Hokkaido, Japan[4]; and Division of Emerging Infectious Diseases, Department of Internal Medicine, Tohoku University, Japan[5]

Received 11 November 2010/Returned for modification 18 November 2010/Accepted 4 February 2011

For the last decade China has occupied second place, after India, among the top five countries with high burdens of tuberculosis (TB). Heilongjiang Province is located in northeastern China. The prevalence of drug-resistant TB in Heilongjiang Province is higher than the average level in China. To determine the transmission characteristics of *Mycobacterium tuberculosis* strains isolated in this area and their genetic relationships, especially among the Beijing family strains, we investigated their genotypes. From May 2007 to October 2008, 200 *M. tuberculosis* isolates from patients presenting pulmonary TB were analyzed by molecular typing using PCR-based methods: spacer-oligonucleotide typing (spoligotyping), Beijing family-specific PCR (detection of the deletion of region of difference 105 [RD105]), and mycobacterial interspersed repetitive-unit-variable-number tandem-repeat (MIRU-VNTR) analysis. Different combinations of MIRU-VNTR loci were evaluated to define the genotypes and clustering characteristics of the local strains. We found that Beijing family strains represented 89.5% of the isolates studied. However, the rates of multidrug-resistant (MDR) *M. tuberculosis* among Beijing and non-Beijing family strains were not statistically different. The 15-locus set is considered the optimal MIRU-VNTR locus combination for analyzing the *M. tuberculosis* strains epidemic in this area, while the 10-locus set is an ideal set for first-line molecular typing. We found that the clustering rate of all the *M. tuberculosis* isolates analyzed was 10.0% using the 15-locus set typing. We conclude that the Beijing family genotype is predominant and that highly epidemic TB and MDR TB are less likely associated with the active transmission of *M. tuberculosis* in the study area.

Tuberculosis (TB) remains a major public health threat worldwide. China has occupied second place, after India, among the top five high-burden countries for the last decade (http://www.who.int/tb/en). Although both the incidence and prevalence of TB in China have shown a steady decline in recent years, it remains a leading notifiable infectious disease (http://www.moh.gov.cn). Currently, the spread of drug-resistant TB, especially multidrug-resistant (MDR) TB, in China, presents a major challenge. The most up-to-date data from the World Health Organization (WHO) indicates that the rate of MDR TB in China was 8.3% (the rates of primary and acquired MDR TB were 5.7% and 25.6%, respectively) in 2007 (50), significantly higher than the global average rate (3.6%). The higher levels of TB prevalence and drug resistance have become the main public health concern of the Chinese government.

Heilongjiang Province, located in northeastern China, is one of the regions where the prevalence of both TB and drug-resistant TB is higher than the average level in China. The most recently updated epidemiological data, from 2007 to 2008, show that the rates of primary and acquired MDR TB were 18.3% and 37.8%, respectively, in Heilongjiang Province (our unpublished data). The reasons for the high prevalence and drug resistance of TB in Heilongjiang Province are still unknown and should be investigated to facilitate control of the TB epidemic in this area and throughout China.

In several Asian countries with high TB rates, a unique genotype of *Mycobacterium tuberculosis*, known as the Beijing family genotype, has been found to be the dominant genotype (3, 17, 34). During the last decade, Beijing family strains have been spreading in various geographic locations worldwide and now account for more than a quarter of all TB cases worldwide (12). Possible associations of the epidemic caused by this genotype with its drug resistance (1, 41) and its high adaptability to the host intracellular environment (8) have been reported. In China, Beijing family strains have spread widely; however, the proportion of Beijing family strains in Heilongjiang Province remains unknown. It is thus unclear if the high prevalence and high drug resistance of epidemic TB are directly related to the spread of Beijing family strains. The answers to these

* Corresponding author. Mailing address: Department of Microbiology, Harbin Medical University, 194 Xuefu Road, Harbin 150081, Heilongjiang Province, China. Phone and fax: 86 451 86685122. E-mail: yfrling@yahoo.com.
† J.W., Y.L., and C.-L.Z. contributed equally to this work.
‡ Present address: Dalian University Affiliated Xinhua Hospital, Dalian, China.
▽ Published ahead of print on 16 February 2011.

TABLE 1. The profile of spoligotypes and RD105 deletion of the *M. tuberculosis* isolates (n = 44)

SIT no.[a]	Spoligotype[b]	Label	No. of isolates[c]	RD105 deletion
1	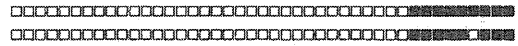	Beijing	39	+
190		Beijing	1	+
1793		Undesignated	1	−
—		New	1 (2460)	+
—		New	1 (2488)	−
—	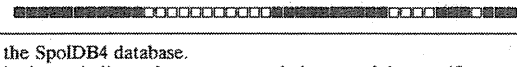	New	1 (2495)	−

[a] —, unassigned in the SpolDB4 database.
[b] The black and white boxes indicate the presence and absence of the specific spacer, respectively.
[c] The identification number of the isolate is given in parentheses.

questions would be very helpful in achieving effective control of TB in Heilongjiang Province as well as throughout China.

To determine the spreading characteristics and the genetic relationships among the *M. tuberculosis* isolates in a given geographic region, a suitable genotyping method is the most important means, i.e., one that is discriminatory, economical, and reproducible. Spacer-oligonucleotide typing (spoligotyping) is a PCR-based method which is simple, highly reproducible, and applicable to a digital format (22). Spoligotyping possesses the most features of an ideal typing method and is the gold standard for identifying strains as belonging to the Beijing family. However, due to the genetic homogeneity of this family, this method is uninformative in the areas where the Beijing family is prevalent (47) and is therefore limited to use as a first-line typing method.

A genotyping method based on mycobacterial interspersed repetitive unit-variable-number tandem repeats (MIRU-VNTR), which is technically flexible to facilitate interlaboratory comparison and database management, is well accepted and has recently been adapted to high-throughput techniques (7, 39). The digital format of MIRU-VNTR patterns makes this method suitable for the global study of the molecular epidemiology of *M. tuberculosis*. A number of studies have investigated the usefulness of different VNTR loci for typing *M. tuberculosis* and have shown that the discriminatory power of this method may be comparable to that of IS*6110* typing, which is the most reliable method for the genetic differentiation of *M. tuberculosis* isolates (33, 38). Because Beijing family strains are prevalent in many developing areas of Asia, where resources are definitely limited, MIRU-VNTR typing would be the best choice here to study the molecular epidemiology of *M. tuberculosis* strains.

Because TB, especially drug-resistant TB, constitutes a heavy burden in Heilongjiang Province, it is important to understand the possible spreading mechanisms of *M. tuberculosis* and particularly drug-resistant TB. In the present study, we conducted the genotyping of *M. tuberculosis* isolates to determine the prevalence of Beijing family strains and the genotypes of *M. tuberculosis* isolates in Heilongjiang Province using MIRU-VNTR analysis. The appropriate VNTR locus combination for genotyping the *M. tuberculosis* isolates in our area was also evaluated and optimized.

MATERIALS AND METHODS

Mycobacterial specimens. The study included 200 *M. tuberculosis* samples isolated between May 2007 and October 2008 from 200 patients from various regions of Heilongjiang Province who had been diagnosed with pulmonary TB in the Harbin Chest Hospital. All the patients were HIV-1 negative. The average age of the patients was 49.1 years, and 71.5% (143/200) were male. *M. tuberculosis* H37Rv was used as the reference strain.

DNA extraction and molecular identification of *M. tuberculosis* isolates and RD105 deletion detection. Mycobacterial cultures were obtained from clinical specimens after incubation in a BACTEC Mycobacterium Growth Indicator Tube (MGIT) 960 Automated System (Becton Dickinson). The cultures were inactivated by 70% ethanol for 2 h (9). DNA was extracted using lysozyme and the phenol-chloroform method (46). Molecular identification of the mycobacterial isolates was performed based on PCR amplification of the 16S rRNA gene and the Rv0577, Rv2073c, and Rv3120 genes (15). Rv2073c amplification was modified as follows: PrimeSTAR HS DNA polymerase (TakaRa, China) was used instead of *Taq* polymerase, and 2 μl of dimethyl sulfoxide was added to ensure good amplification. The amplification cycle was 5 min at 98°C followed by 25 cycles of 1 min at 98°C, 5 s at 65°C, and 40 s at 72°C, with a final 10 min at 72°C. The identification of genomic deletions in region of difference 105 (RD105) was performed by PCR as previously described (14, 26). Briefly, each PCR mixture was prepared in a volume of 20 μl containing 50 ng of DNA, 0.25 U of *Taq* polymerase (TakaRa, China), a 0.2 mM concentration of each deoxynucleoside triphosphate (dNTP), and 0.2 μM (each) primer. The amplification cycle was 10 min at 94°C followed by 25 cycles of 1 min at 94°C, 1 min at 60°C, and 1 min at 72°C, with a final step for 10 min at 72°C.

Spoligotyping. Spoligotyping of the isolates was performed as described by Kamerbeek et al. (22). The direct repeat (DR) region was amplified with the primer pair, and the PCR products were hybridized to a set of 43 oligonucleotide probes corresponding to each spacer, which were covalently bound to a mem-

TABLE 2. Allelic diversity of different MIRU-VNTR loci[a]

MIRU-VNTR locus	No. of alleles (range)		h	
	Isolate set 1	Isolate set 2	Isolate set 1	Isolate set 2
QUB26	7 (4–10)	8 (3–10)	0.706	0.581
QUB11b	6 (3–8)	9 (0–8)	0.644	0.730
MIRU31	6 (2–7)	7 (2–8)	0.599	0.500
MIRU16	4 (2–6)	4 (2–6)	0.520	0.230
MIRU4	5 (1–5)	6 (0–5)	0.517	0.260
MIRU26	5 (4–9)	8 (3–10)	0.467	0.649
Mtub4	4 (2–5)	6 (0–5)	0.413	0.463
MIRU40	5 (1–5)	6 (1–6)	0.373	0.358
Mtub21	6 (1–8)	9 (1–9)	0.307	0.493
Mtub39	4 (1–6)	6 (1–6)	0.229	0.243
MIRU10	4 (1–4)	4 (1–4)	0.229	0.300
Mtub30	4 (2–5)	4 (2–5)	0.191	0.267
Mtub29	3 (3–5)	5 (2–6)	0.189	0.138
MIRU39	3 (1–3)	4 (1–4)	0.149	0.388
ETR A	2 (3–4)	7 (0–6)	0.146	0.329
QUB4156	2 (2–4)	5 (0–4)	0.107	0.182
ETR C	3 (2–5)		0.068	
ETR B	2 (1–2)		0.066	
MIRU23	1 (5)		0	

[a] Set 1 consists of 44 isolates obtained from May 2007 to November 2007. Set 2 consists of 200 isolates obtained from May 2007 to October 2008.

TABLE 3. The cumulative HGDI with successive addition of each MIRU-VNTR locus

Locus combination[a]	VNTR locus (h)[b]	No. of patterns	No. of clusters	No. of clustered isolates	No. of isolates in each cluster	Clustering rate (%)	HGDI (cumulative)
1	QUB11b (0.730)						
2	MIRU26 (0.649)	35	19	184	2–41	82.5	0.9042
3	QUB26 (0.581)	84	33	149	2–23	58.0	0.9686
4	MIRU31 (0.500)	112	33	121	2–18	44.0	0.9808
5	Mtub21 (0.493)	126	33	107	2–16	37.0	0.9867
6	Mtub4 (0.463)	135	30	95	2–15	32.5	0.9888
7	MIRU39 (0.388)	150	23	73	2–14	25.0	0.9913
8	MIRU40 (0.358)	159	18	59	2–12	20.5	0.9935
9	ETR A (0.329)	164	16	52	2–12	18.0	0.9943
10	MIRU10 (0.300)	169	14	45	2–12	15.5	0.9950
11	Mtub30 (0.267)	169	14	45	2–12	15.5	0.9950
12	MIRU4 (0.260)	176	12	36	2–10	12.0	0.9967
13	Mtub39 (0.243)	178	10	32	2–10	11.0	0.9968
14	MIRU16 (0.230)	179	11	32	2–8	10.5	0.9976
15	QUB4156 (0.182)	180	10	30	2–8	10.0	0.9977
16	Mtub29 (0.138)	180	10	30	2–8	10.0	0.9977

[a] The successive addition of each VNTR locus.
[b] The h value represents the diversity determined from the 200 isolates.

brane (22). Spoligotypes in binary format were compared with the SpolDB4 database, and the spoligotype international type (SIT) numbers and the clades were also determined (4).

MIRU-VNTR typing. To identify a suitable MIRU-VNTR locus set for genotyping *M. tuberculosis* isolates in this area, 19 loci were selected for analyzing the first set of 44 *M. tuberculosis* isolates (38). The PCR mixture and conditions were the same those for the RD105 deletion identification described above. Genomic DNA of the H37Rv strain and sterile distilled water were used as the positive and negative controls, respectively. PCR products were analyzed on a 1.5% agarose gel against a 100-bp DNA ladder (TakaRa, China), and the copy number at each locus was calculated using a Quantity 1 gel imaging system (Tanon, China). The MIRU-VNTR allelic diversity (h) at a given locus was calculated as follows: $h = 1 - \Sigma x_i^2[n/(n-1)]$, where x_i is the frequency of the ith allele at the locus, and n is the number of isolates (35). The discrimination of the locus combination was calculated using the Hunter-Gaston discriminatory index (HDGI) (16):

$$\mathrm{HGDI} = 1 - \frac{1}{N(N-1)}\sum_{j=1}^{s} n_j(n_j - 1)$$

where N is the total number of isolates in the typing method, s is the number of distinct patterns discriminated by MIRU-VNTR, and n_j is the number of isolates belonging to the jth pattern.

Phylogenetic and cluster analysis. We used the R software, version 2.11.1 (http://cran.r-project.org), for phylogenetic and cluster analysis. A dendrogram was produced from the MIRU-VNTR genotypes of the 200 *M. tuberculosis* isolates. First, the repeat numbers of MIRU-VNTR genotypes were standardized based on a z-score normalization. Then, a similarity coefficient matrix of the *M. tuberculosis* isolates was obtained by calculating the Euclidean distances between isolates from the standardized data. Finally, clustering was performed, and a phylogenetic tree was constructed using Ward's parameter with the matrix. The *M. tuberculosis* isolates analyzed in this study were classified into two groups, characterized by clustered and nonclustered *M. tuberculosis* isolates. A molecular cluster was defined as two or more *M. tuberculosis* isolates having identical genetic patterns as determined by MIRU-VNTR genotyping. The isolates with unmatched genetic profiles were considered nonclustered strains. Assuming that one patient from each cluster corresponded to the index case at the origin of infection, the clustering rate was calculated using the following formula: clustering rate $= (n_c - c)/n$, where n_c is the total number of clustered isolates, c is the number of isolate clusters, and n is the total number of isolates in the sample (37).

Statistical analysis. Associations among multiple categorical variables were assessed using R, version 2.11.1, by a chi-square test or Fisher's exact test when the theoretical frequency was less than five. Two-by-two tables were assessed by a chi-square test (here, Yates' continuity correction was needed when the value was less than five), and results were expressed as odds ratios (OR) with 95% confidence intervals (95% CI). The agreement between spoligotyping and RD105 deletion typing was assessed using kappa statistics; the agreement was considered good for values of kappa above 0.75. P values of <0.05 were considered statistically significant.

RESULTS

Epidemic of Beijing family strains in Heilongjiang Province. During the study period, 200 *M. tuberculosis* isolates identified using both the BACTEC 960 automated system and molecular methods were collected. First, we analyzed the correlation between spoligotyping and RD105 deletion for the identification of the Beijing genotype using 44 isolates collected from May 2007 to November 2007. Among the 44 *M. tuberculosis* isolates, spoligotypes of 41 isolates were classified into three designated SITs according to the SpolDB4 database (Table 1). Among these, 40 isolates were Beijing family strains. The most frequent genotype (39/41) was the typical Beijing spoligotype SIT1, which has only spacers 35 to 43; the only other Beijing genotype belonged to spoligotype SIT190. One isolate, with an SIT number of 1793, was not designated in the database. The remaining three isolates showed new spoligotypes, which were not registered in SpolDB4 database. Interestingly, one isolate (2460) showed a unique genotype with only two spacers, 35 and 36. We found that 40 isolates lacking RD105 exhibited Beijing family spoligotypes (Table 1). The *M. tuberculosis* isolate 2460 also lacked RD105. The results of the kappa statistics analysis showed that the agreement of spoligotyping and RD105 deletion detection in identifying the Beijing family genotype was high ($\kappa = 0.8451$). Subsequently, instead of using spoligotyping, RD105 deletions in the other 156 *M. tuberculosis* strains were examined, and we found that 179 of the 200 isolates (89.5%) had the Beijing family genotype, while 21 (10.5%) were non-Beijing family strains.

Optimal combination of MIRU-VNTR loci for genotyping *M. tuberculosis* isolates in Heilongjiang Province. First, to evaluate and determine the most suitable loci for genotyping the *M. tuberculosis* isolates epidemic in Heilongjiang Province, we analyzed 19 MIRU-VNTR loci, which had been previously identified as a suitable locus combination for genotyping *M. tuberculosis* isolates in the regions where the Beijing family is

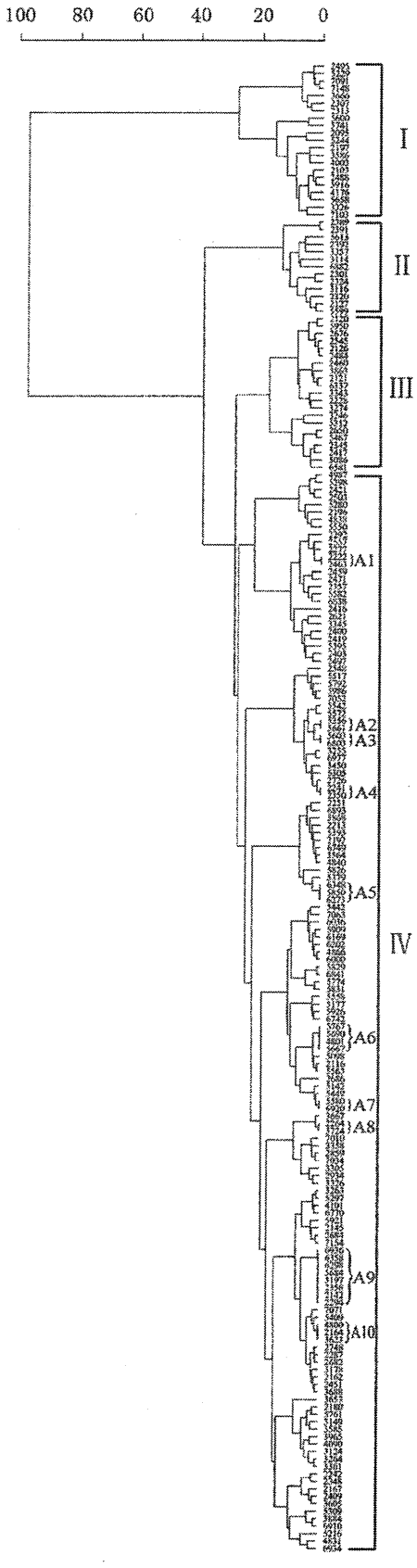

dominant (19, 27) (Table 2). The allelic diversity (h) of the first set of 44 *M. tuberculosis* isolates at each MIRU-VNTR locus varied significantly. Among the 19 loci, the allelic diversity for 2 loci (QUB11b and QUB26) exceeded 0.6, suggesting that they are highly discriminating (30). Seven loci (MIRU4, MIRU16, MIRU26, MIRU31, MIRU40, Mtub21, and Mtub4) showed moderate discrimination ($0.3 \leq h \leq 0.6$), but ETR C ($h = 0.068$) and ETR B ($h = 0.066$) were less polymorphic. Diversity was not observed for the MIRU23 locus ($h = 0$). Thus, the loci ETR C, ETR B, and MIRU23, having discriminatory powers of less than 0.1, were excluded from the subsequent MIRU-VNTR analysis.

Next, we analyzed the 200 *M. tuberculosis* isolates collected from May 2007 to October 2008 using the remaining 16 MIRU-VNTR loci. All 16 loci displayed an allelic diversity similar to the original 19 loci (Table 2). The highest diversity among the 200 isolates was observed at QUB11b ($h = 0.730$), and the lowest diversity was observed at Mtub29 ($h = 0.138$). The HGDI of the 16-locus set was as high as 0.9977. However, because the 16-locus procedure still did not meet the requirements of cost and labor expenditure for high-throughput genotyping, we then tried to optimize the locus combination while minimizing the number of loci. Based on the allelic diversity of each MIRU-VNTR locus, the cumulative HGDI of the locus combination by successive addition of a locus was compared (Table 3). The cumulative HGDI and clustering rate of the 10-locus set were equal to that of the 11-locus set (HGDI, 0.9950; clustering rate, 15.5%); they were also the same for the 15- and the 16-locus sets (HGDI, 0.9977; clustering rate, 10.0%). The set of the first seven loci with the highest allelic diversity gave an HGDI of 0.9913 and a clustering rate of 25.0%.

VNTR profiles and genotypes of the *M. tuberculosis* isolates in Heilongjiang Province. The MIRU-VNTR genotyping results showed that the 200 isolates were classified into 180 genotypes. A total of 170 isolates had unique patterns, while the remaining 30 isolates were in 10 clusters. A dendrogram was constructed based on the genotypes of 200 isolates using 16 loci (Fig. 1). The isolates were divided into four groups based on phylogenetic clustering and genotypic characteristics. Groups I to IV contained 21, 13, 21, and 145 isolates, respectively. Among the 179 Beijing family isolates, 144 (99.3%) were in group IV; the remaining 35 isolates were in groups I, II, and III ($P < 0.0001$), and all the clustered isolates were in group IV ($P = 0.0018$), suggesting that the distributions of the Beijing family isolates and clustered isolates were distinctive among the four groups (Table 4).

Characteristics of the clustered isolates. Thirty Beijing family isolates (30/179, or 16.8% of the Beijing family strains) were determined to be in 10 clusters (A1 to A10), with the clustering rate of 10.0% based on 15-locus MIRU-VNTR patterns. In contrast, none of 21 non-Beijing family isolates were clustered (OR, 0; 95% CI, 0 to 1.024; $P = 0.087$) (Table 5). Most of the

FIG. 1. Dendrogram of 200 *M. tuberculosis* isolates from Heilongjiang Province. The phylogenetic tree was produced from the MIRU-VNTR genotypes which were derived from 16 of the 19 loci by excluding ETR B, ETR C, and MIRU23. A1 to A10, cluster names.

TABLE 4. Differences of *M. tuberculosis* characteristics among the four subgroups

Isolate characteristic	Total no. of isolates	No. (%) of isolates by subgroup[a]				*P* value[b]
		I (n = 21)	II (n = 13)	III (n = 21)	IV (n = 145)	
Resistance						
Streptomycin	85	9 (42.9)	6 (46.2)	8 (38.1)	62 (42.8)	0.9704*
Isoniazid	92	9 (42.9)	8 (61.5)	7 (33.3)	68 (46.9)	0.4317*
Rifampin	55	4 (19.0)	7 (53.8)	3 (14.3)	41 (28.3)	0.0815
Ethambutol	48	4 (19.0)	6 (46.2)	3 (14.3)	35 (24.1)	0.2070
MDR	51	4 (19.0)	6 (46.2)	2 (9.5)	39 (26.9)	0.1032
Four-drug susceptibility	77	8 (38.1)	3 (23.1)	9 (42.9)	57 (39.3)	0.6786*
Four-drug resistance	23	2 (9.5)	3 (23.1)	1 (4.8)	17 (11.7)	0.4402
Obtained from a patient with acquired TB	126	17 (81.0)	9 (69.2)	11 (52.4)	89 (61.4)	0.2294
Obtained from a patient with hemoptysis	169	15 (71.4)	9 (69.2)	20 (95.2)	125 (86.2)	0.0562
Beijing strain	179	3 (14.3)	12 (92.3)	20 (95.2)	144 (99.3)	<0.0001
Clustered	30	0 (0)	0 (0)	0 (0)	30 (20.7)	0.0018

[a] n, number of isolates in the subgroup.
[b] Values marked with an asterisk were determined by a chi-square test; other values were determined by a Fisher's exact test.

clusters were small: six (A1 to A4, A7, and A8) contained only two members; two (A5 and A10) contained three members; cluster A6 contained four members. The largest cluster, A9, contained eight members. In addition, the clustering rates of the two periods, May 2007 to May 2008 (106 isolates) and June 2008 to October 2008 (94 isolates), were 6.4% and 12.8%, respectively (OR, 0.3240; 95% CI, 0.1161 to 0.8265; P = 0.0088).

To determine if there was any correlation between the clustering characteristics and the geographical origins of the isolates, we investigated the home addresses of the patients in the clusters from the available medical records. We found that the isolates belonging to clusters A2 and A7 were scattered throughout the Heilongjiang Province while clusters A3 to A6, A9, and A10 were registered in Harbin City.

Drug susceptibility patterns of the *M. tuberculosis* isolates in Heilongjiang Province. To determine the association between drug resistance patterns and genotypic characteristics, drug susceptibility to the four first-line antituberculosis drugs, i.e., streptomycin, isoniazid, rifampin, and ethambutol, was examined using an automated BACTEC MGIT 960 SIRE system (Becton Dickinson). A total of 77 isolates (38.5%) were susceptible to all four drugs; 123 (61.5%) were resistant to at least one drug, and 51 (41.5%) were MDR *M. tuberculosis* (Tables 4 and 5). The drug susceptibility patterns of the isolates among the four genotype groups were not significantly different (Table 4). Of the 51 MDR *M. tuberculosis* isolates, 48 isolates were found to be the Beijing family strains, and 3 were non-Beijing family strains. Of the Beijing family strains, 26.8% (48/179) were MDR, and 14.3% (3/21) of the non-Beijing family strains were MDR. The rates of MDR *M. tuberculosis* among Beijing and non-Beijing family strains were not statistically different (OR, 0.4564; 95% CI, 0.0824 to 1.6670; P = 0.2127). Resistance to at least one drug was observed more frequently among Beijing family strains (63.1%, or 113/179) than among non-Beijing family strains (47.6%, or 10/21), but the difference was not statistically significant (OR, 1.8771; 95% CI, 0.6828 to 5.2244; P = 0.1670) (Table 5).

DISCUSSION

The Beijing family strains currently prevail throughout China. RD105 deletion has recently been reported to serve as a genetic marker for Beijing family strains (44), and several

TABLE 5. Differences of *M. tuberculosis* characteristics between Beijing and non-Beijing family

Isolate characteristic	Total no. of isolates	No. (%) of isolates[a]		OR	95% CI	*P* value[b]
		Beijing (n = 179)	Non-Beijing (n = 21)			
Resistance						
Streptomycin	85	78 (43.6)	7 (33.3)	0.6488	0.2110–1.8176	0.3691
Isoniazid	92	84 (46.9)	8 (38.1)	0.6972	0.2381–1.9189	0.4423
Rifampin	55	52 (29.1)	3 (14.3)	0.4086	0.0739–1.4876	0.1517
Ethambutol	48	45 (25.1)	3 (14.3)	0.4978	0.0898–1.8235	0.4056*
MDR	51	48 (26.8)	3 (14.3)	0.4564	0.0824–1.6670	0.2127
Four-drug susceptibility	77	66 (36.8)	11 (52.4)	1.8771	0.6828–5.2244	0.1670
Four-drug resistance	23	21 (11.7)	2 (9.5)	0.7928	0.0837–3.6902	0.9510*
Obtained from a patient with acquired TB	126	109 (60.9)	17 (90.0)	2.7174	0.8390–11.5638	0.0717
Obtained from a patient with hemoptysis	169	153 (85.5)	16 (76.2)	1.8323	0.4830–5.8459	0.4275*
Clustered	30	30 (16.8)	0 (0)	0	0–1.0241	0.0869*

[a] n, number of isolates in the group.
[b] Values marked with an asterisk were determined by a continuity-adjusted chi-square test; other values were determined by a chi-square test.

studies have used this method to identify them (6, 26, 45). It is financially economical, labor saving, and especially suitable for high-throughput analysis. In this study, we found good agreement between RD105 deletion detection and spoligotyping. One strain (2460) showed a novel spoligotype containing only spacers 35 and 36 and an RD105 deletion. According to the definition of the Beijing family spoligotype, these strains contain at least three spacers among direct repeats 35 to 43; however, strain 2460 can be included in the Beijing family because it lacks RD105.

We found that 89.5% of the *M. tuberculosis* isolates in Heilongjiang Province were Beijing family strains. This genotype accounts for 80 to 90% of the *M. tuberculosis* strains currently epidemic in the Beijing area (19); it is also prevalent in Ningxia (67%), Shanghai (89%), Zhejiang (70%), Tianjin (91.7%), and Guangxi (55.3%) but less prevalent in Guangdong (25%) (5, 24, 25, 36, 48). Hence, Heilongjiang Province is one of the regions where the proportion of the Beijing genotype is the highest. This genotype is thought to be associated with drug resistance (1, 10, 23, 41). However, less association has been reported in other geographic settings (2, 3, 20, 43). In the present study, the statistical analysis showed that there was no difference between the Beijing and non-Beijing genotype strains in drug resistance patterns, indicating that the Beijing genotype is less likely to be associated with the high prevalence of drug resistance and *M. tuberculosis* TB in our area.

Molecular typing by MIRU-VNTR has been used in epidemiology studies, and its stability is adequate for tracking recent transmission and distinguishing relapses and reinfections (39). Currently, the system based on 12 loci (29) is most widely used among the different sets of MIRU-VNTR loci. However, it is not effective for the analysis of clustered isolates (7). Other sets of MIRU-VNTR loci, such as the 14-locus set and the 15-locus set, have improved the discrimination of unrelated isolates (23, 38). An optimized set of 24 loci has also been defined; however, not all 24 loci are required for genotyping *M. tuberculosis* strains in any given situation (38) as the number of loci required depends on the lineage known to be prevalent in the investigated area.

In the present study, we found that the 16 of the 19 loci had high discriminatory diversity. This 16-locus set showed strong discriminatory power in analyzing the *M. tuberculosis* strains in our area (HGDI of 0.9977). Because the ability of the different locus combinations to differentiate the *M. tuberculosis* strains varied, we evaluated various sets of MIRU-VNTR loci to identify a minimal subset that provided discrimination comparable to that of the 16 loci. We found that the locus Mtub29 could be excluded from the set because the HGDI and clustering rate of the remaining 15 loci were the same as those of the 16 loci. The HGDI and the clustering rate of a 10-locus set were comparable to those of the 16-locus set. Therefore, we suggest that this 10-locus set be used as a first-line set for genotyping *M. tuberculosis* isolates in Heilongjiang Province, especially for routine epidemiological investigation and large-scale genotyping. Comparing the HGDI and the clustering rate of this locus set with those of various locus sets reported in other areas of China, we found that the discriminatory power of the 15-locus set used in the present study was the highest and that the clustering rate was the lowest (Table 6).

However, MIRU-VNTR loci showed variation in the ability to differentiate Beijing genotype strains from different geographical areas. Trying to explore the loci showing high discriminatory power among Beijing genotype strains in various areas of the world (Table 7), we found that at least 11 and 14 loci showed high enough diversity among the locally circulating Beijing genotype strains in China and Japan, respectively. Therefore, we recommend them as the predominant candidates (Table 7, underlined median *h* value for China and Japan). Since the Beijing genotype is dominant in China and Japan, we also suggest taking the 14 loci that show high diversity among the strains epidemic in the two countries as the predominant candidates for Asia (Table 7, underlined Asian median values). Meanwhile, the loci showing very low diversity (Table 7, boldface), 11 from China and 9 from Japan, may not need to be included for future studies. However, there are still some loci that showed high variation in differentiating Beijing genotype strains. For example, the loci MIRU10 and MIRU16 showed moderate diversity in Hong Kong and Gansu but low diversity in the other areas of China. The locus VNTR4120 was highly discriminatory in Japan (*h* of 0.902) but less discriminatory in China (*h* of 0.092).

In Japan, most of the loci reported showed comparatively high discriminatory power; therefore, considering labor and cost, some loci with moderate *h* values (>0.3) may not need to be included. Russia is much different from Japan and China in allelic diversity of the MIRU-VNTR loci, and the *h* values of most loci are much lower than those in China and Japan. This difference may imply that the loci which are suitable for genotyping the isolates epidemic in Asia may not be suitable for genotyping isolates in Russia.

Active transmission of drug-resistant *M. tuberculosis* strains in a community is an emerging problem. It is generally assumed that the proportion of clustered strains in a population reflects the level of active transmission (11, 28). The present study using 15 loci showed that the clustering rate in Heilongjiang Province is 10.0%, which is lower than the rates reported in other areas (Table 6). Though some loci that show moderate or high discriminatory power in other areas were not included in the present study, omitting them will not increase the clustering rate in this area because the loci may decrease the clustering trend of the strains by decreasing the diversity. The

TABLE 6. Discriminatory index of different locus sets used in various regions of China and the clustering rates

Area	Locus set	Clustering rate (%)	HGDI	Reference
Hong Kong	17 loci	17.4	0.9900	23
Shanghai	16 loci	16.1	0.9982	52
	7 loci	25.0	0.9957	
Beijing	24 loci	15.3	0.9920	19
	15 loci	18.1	0.9900	
	12 loci	59.7	0.7880	
Fujian	12 loci	17.1	0.9808	18
Gansu	15 loci	42.1		42
Zhejiang	15 loci	30.0	0.9905	49
Eight regions	12 loci	33.5	0.9780	13
Five regions	19 loci	15.7	0.9949	27
Heilongjiang	15 loci	10.0	0.9977	This study
	10 loci	15.5	0.9950	
	7 loci	25.0	0.9913	

TABLE 7. Allelic diversity of different MIRU-VNTR loci for differentiating *M. tuberculosis* Beijing family strains in different areas

Locus	Allelic diversity (h) by region[a]														
	Russia[b]			Japan[c]				China[d]							Median for Asia
	St. Petersburg (n = 48)	West Siberia (n = 51)	Median	Kobe (n = 181)	Japan (n = 240)	Chiba (n = 185)	Median	Beijing (n = 72)	Shanghai (n = 189)[e]	Hong Kong group 1 (n = 51)	Hong Kong group 2 (n = 243)	Gansu (n = 202)	Heilongjiang (n = 179)	Median	
VNTR4120	0.370		0.370	0.902	0.902	0.882	0.902		0.092*					0.092	0.892
QUB3232	0.729		0.729	0.880	0.909	0.813	0.880				0.804			0.804	0.847
VNTR3820	0.542		0.542	0.800	0.871	0.817	0.817		0.821					0.821	0.819
QUB11b	0.205	0.210	0.208	0.772	0.815	0.763	0.772	0.651	0.689	0.618	0.669		0.704	0.669	0.697
QUB18		0.740	0.740			0.629	0.629		0.607	0.740	0.488			0.607	0.618
Mtub24					0.591	0.614	0.603		0.223					0.223	0.591
QUB26	0.636	0.780	0.708	0.741	0.764	0.215	0.741	0.518	0.630	0.299	0.314		0.607	0.518	0.563
Mtub21	0.330	0.110	0.220	0.393	0.598	0.537	0.537	0.556	0.544			0.690	0.396	0.550	0.544
QUB11a				0.685	0.752	0.535	0.685		0.538	0.384	0.514			0.514	0.537
QUB3336				0.487	0.642	0.482	0.487				0.214			0.214	0.485
QUB4156	0.082		0.082	0.611	0.623	0.603	0.611	0.395	0.469		0.167		0.182	0.289	0.469
Mtub4	0.000		0.000	0.459	0.468	0.581	0.468	0.306	0.266				0.391	0.306	0.425
MIRU26	0.520		0.520	0.383	0.314	0.283	0.314	0.353	0.614	0.200		0.560	0.596	0.560	0.368
QUB1895				0.364	0.337	0.468	0.364		0.365	0.229	0.206			0.229	0.351
VNTR2372					0.595	0.345	0.470		0.177*					0.177	0.345
QUB15					0.537	0.629	0.583		0.032*		0.132			0.082	0.335
MIRU31	0.160	0.000	0.080	0.322	0.270	0.379	0.322	0.169	0.328		0.156	0.370	0.395	0.328	0.325
ETR F					0.237	0.499	0.368		0.290					0.290	0.290
MIRU10	0.082		0.082	0.419	0.431	0.291	0.419	0.144	0.239	0.377		0.160	0.154	0.160	0.265
MIRU40	0.122	0.390	0.256	0.327	0.229	0.473	0.327	0.194	0.147*	0.196		0.350	0.292	0.196	0.261
MIRU16	0.082		0.082	0.310	0.258	0.421	0.310	0.068	0.131	0.058		0.580	0.200	0.131	0.229
ETR A	0.158	0.000	0.079	0.147	0.223	0.165	0.165	0.232	0.031*	0.201	0.188	0.280	0.238	0.217	0.201
Mtub39	0.000	0.000	**0.000**	0.186	0.215	0.271	0.215	0.171	0.061*			0.120	0.174	0.146	0.174
MIRU39	0.000		**0.000**	0.221	0.156	0.160	0.160	0.119	0.141	0.320	0.040	0.100	0.290	0.141	0.158
Mtub30	0.042		0.042	0.403	0.379	0.210	0.379	0.068	0.091*			0.090	0.133	**0.090**	0.133
Mtub29	0.087	0.180	0.134	0.043	0.095	0.103	**0.095**	0.119	0.061*				0.123	**0.119**	**0.103**
MIRU23	0.000	0.000	**0.000**	0.176	0.158	0.124	0.158	0.014	0.061*			0.030		**0.030**	**0.093**
QUB5(MIRU27)	0.000		**0.000**	0.115	0.081	0.074	**0.081**	0.014	0.031*			0.100		**0.031**	**0.078**
MIRU4	0.000		**0.000**	0.086	0.049	0.000	**0.049**	0.120	0.061	0.019	0.072		0.212	**0.061**	**0.067**
MIRU20	0.120		**0.120**	0.022	0.065	0.063	**0.063**	0.014	0.061*					**0.038**	**0.061**
ETR C	0.042	0.000	**0.021**	0.022	0.057	0.063	**0.057**	0.094		0.165	0.057	0.000		**0.076**	**0.057**
Mtub34	0.000		**0.000**	0.066	0.033	0.000	**0.033**	0.014	0.089*					**0.052**	**0.033**
QUB23					0.025		0.025				0.016			0.016	0.021
ETR B	0.000		**0.000**	0.033	0.017	0.032	**0.032**	0.014	0.000*	0.000	0.064	0.020		**0.014**	**0.019**
VNTR0569						0.011	0.011		0.000*					0.000	0.006
QUB1451				0.033			0.033		0.000*		0.008			0.004	0.008
MIRU2	0.000		**0.000**	0.000	0.008	0.000	**0.000**	0.000	0.000*					**0.000**	**0.000**
MIRU24	0.000		**0.000**	0.000	0.000	0.042	**0.000**	0.000	0.000*					**0.000**	**0.000**
ETR E		0.000	**0.000**												0.000

[a] n, number of isolates; underlining, corresponding locus was recommended; boldface, corresponding locus was not recommended.
[b] See the following references: for St. Petersburg, 31; for West Siberia, 40.
[c] See the following references: for Kobe, 17; for Japan, 32; for Chiba, 51. The Japan strains were from a drug resistance survey in Japan in 2002.
[d] See the following references: for Beijing, 19; for Shanghai, 52; for Hong Kong group 1, 23; for Hong Kong group 2, 21; and for Gansu, 42. Hong Kong strains were collected in 2001 (group 1) or 2001 to 2003 (group 2).
[e] For values marked with an asterisk, the number of samples was 65.